JACS ARTICLES

Published on Web 08/10/2010

Role of Aromatic Rings in the Molecular Recognition of Aminoglycoside Antibiotics: Implications for Drug Design

Tatiana Vacas,[†] Francisco Corzana,[‡] Gonzalo Jiménez-Osés,[§] Carlos González,[||] Ana M. Gómez,[†] Agatha Bastida,[†] Julia Revuelta,[†] and Juan Luis Asensio[†,*]

Instituto de Química Orgánica General (CSIC), Juan de la Cierva 3, 28006 Madrid, Spain, Departamento de Química, Universidad de La Rioja, UA-CSIC, Logroño, Spain, Departamento de Química Orgánica y Química Física. Universidad de Zaragoza-CSIC, Zaragoza, Spain, and Instituto de Química Física Rocasolano (CSIC), Madrid, Spain

Received May 28, 2010; E-mail: iqoa110@iqog.csic.es

Abstract: Aminoglycoside antibiotics participate in a large variety of binding processes involving both RNA and proteins. The description, in recent years, of several clinically relevant aminoglycoside/receptor complexes has greatly stimulated the structural-based design of new bioactive derivatives. Unfortunately, design efforts have frequently met with limited success, reflecting our incomplete understanding of the molecular determinants for the antibiotic recognition. Intriguingly, aromatic rings of the protein/RNA receptors seem to be key actors in this process. Indeed, close inspection of the structural information available reveals that they are frequently involved in CH/π stacking interactions with sugar/aminocyclitol rings of the antibiotic. While the interaction between neutral carbohydrates and aromatic rings has been studied in detail during past decade, little is known about these contacts when they involve densely charged glycosides. Herein we report a detailed experimental and theoretical analysis of the role played by CH/π stacking interactions in the molecular recognition of aminoglycosides. Our study aims to determine the influence that the antibiotic polycationic character has on the stability, preferred geometry, and dynamics of these particular contacts. With this purpose, different aminoglycoside/aromatic complexes have been selected as model systems. They varied from simple bimolecular interactions to the more stable intramolecular CH/π contacts present in designed derivatives. The obtained results highlight the key role played by electrostatic forces and the desolvation of charged groups in the molecular recognition of polycationic glycosides and have clear implications for the design of improved antibiotics.

Introduction

Aminoglycosides are highly potent, broad-spectrum antibiotics widely used in clinics. These drugs bind specifically to the bacterial decoding site, in the 16S rRNA (A-site), and thereby interfere with the accuracy of protein synthesis, leading to bacterial cell death.[1] Additional targets such as the DIS kissing-loop complex, the Tat-responsive element, and the Rev-responsive element have been identified within the HIV genomic RNA and are also located in different functionally relevant RNA fragments, including self-splicing ribozymes and tRNAs.[2] In addition to interacting specifically with RNA receptors, aminoglycosides are also recognized by the enzymes involved in antibiotic inactivation that play a central role in bacterial resistance processes.[3] These proteins represent primary pharmacological targets.

The emergence during the past decade of high-resolution structural data for aminoglycoside/protein[4] and aminoglycoside/RNA[5] complexes has greatly stimulated the structure-based design of new bioactive derivatives with improved properties.

[†] Instituto de Química Orgánica General.
[‡] Universidad de La Rioja.
[§] Universidad de Zaragoza.
[||] Instituto de Química Física Rocasolano.

(1) (a) Talaska, A. E.; Schacht, J. In *Aminoglycoside Antibiotics: from Chemical Biology to Drug Discovery*, Arya, D. P., Ed.; Wiley.: New York, 2007. (b) Vicens, Q.; Westhof, E. *ChemBioChem* **2003**, *4*, 1018–1023.

(2) (a) Schroeder, R.; Waldsich, C.; Wank, H. *EMBO J.* **2000**, *19*, 1–9. (b) Walter, F.; Vicens, Q.; Westhof, E. *Curr. Opin. Chem. Biol.* **1999**, *3*, 694–704. (c) Sucheck, J. S.; Wong, C. H. *Curr. Opin. Chem. Biol.* **2000**, *4*, 678–686.

(3) (a) Magnet, S.; Blanchard, J. S. *J. Chem. Rev.* **2005**, *105*, 477–497. (b) Smith, C. A.; Baker, E. N. *Curr. Drug Targets* **2002**, *2*, 143–160.

(4) (a) Pedersen, L. C.; Benning, M. M.; Holden, H. M. *Biochemistry* **1995**, *34*, 13305–13311. (b) Fong, D. H.; Berghuis, A. M. *EMBO J.* **2002**, *21*, 2323–2331. (c) Vetting, M. W.; Park, C. H.; Hedge, S. S.; Jacoby, G. A.; Hooper, D. C.; Blanchard, J. S. *Biochemistry* **2008**, *47*, 9825–9835. (d) Maurice, F.; Broutin, I.; Podglajen, I.; Benas, P.; Collatz, E.; Dardel, F. *EMBO Rep.* **2008**, *9*, 344–349. (e) Nurizzo, D.; Shewry, S. C.; Perlin, M. H.; Brown, S. A.; Dholakia, J. N.; Fuchs, R. L.; Deva, T.; Baker, E. N.; Smith, C. A. *J. Mol. Biol.* **2003**, *327*, 491–506.

(5) (a) Carter, A. P.; Clemons, W. M.; Brodersen, D. E.; Morgan-Warren, R. J.; Wimberly, B. T.; Ramakrishnan, V. *Nature* **2000**, *407*, 340–348. (b) Vicens, Q.; Westhof, E. *Chem. Biol.* **2002**, *9*, 747–755. (c) Francois, B.; Rusell, R. J. M.; Murray, J. B.; Aboul-ela, F.; Masquida, B.; Vicens, Q.; Westhof, E. *Nucleic. Acids. Res.* **2005**, *33*, 5677–5690. (d) Mikkelsen, N. E.; Johanson, K.; Virtanen, A.; Kirsebom, L. A. *Nat. Struct. Biol.* **2001**, *8*, 510–514. (e) Freisz, S.; Lang, K.; Micura, R.; Dumas, P.; Ennifar, E. *Angew. Chem., Int. Ed.* **2008**, *47*, 4110–4113. (f) Ennifar, E.; Paillart, J. C.; Marquet, R.; Ehresmann, B.; Ehresmann, C.; Dumas, P.; Walter, P. *J. Biol. Chem.* **2003**, *278*, 2723–2730. (g) Tereshko, V.; Skripkin, E.; Patel, D. J. *Chem. Biol.* **2003**, *10*, 175–187.

10.1021/ja1046439

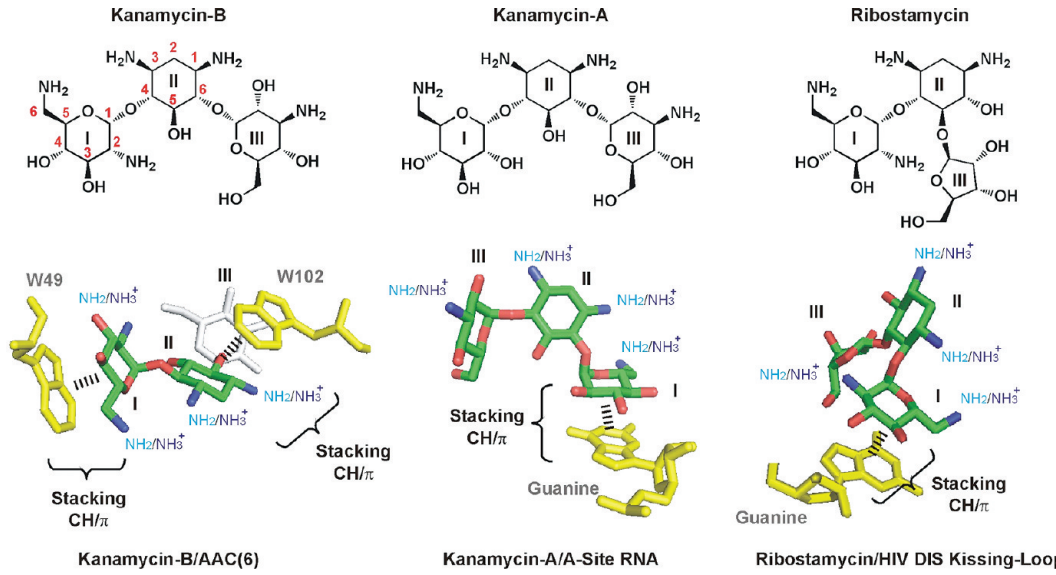

Figure 1. (Top) Schematic representation of kanamycin-B (left panel), kanamycin-A (middle panel), and ribostamycin (right panel). The numbering employed for the different sugar/aminocyclitol units is shown in black. In addition, the numbering employed for the different positions of the I/II fragment is shown in red on the kanamycin-B structure (left panel). (Bottom) CH/π stacking interactions present in their respective complexes with the resistance enzyme AAC(6′) (pdb code 2QIR), the ribosomal A-site RNA (pdb code 2ESI) and the viral HIV DIS kissing-loop (pdb code 2FCZ), according to X-ray data. In the former case (left) the antibiotic unit III is represented in white for clarity. The position of the aminoglycoside NH_2/NH_3^+ groups is highlighted.

More specifically, research has been focused on the preparation of tighter, more specific, and less toxic RNA binders,[6] enzymatic inhibitors,[7] and new drugs not susceptible to enzymatic inactivation.[8] Unfortunately, design efforts have frequently met with limited success, which, in our opinion, partially reflects our limited understanding of the molecular forces that stabilize the aminoglycoside complexes at a fundamental level.

Intriguingly, a detailed inspection of the structural information available reveals that both protein and RNA receptors employ common strategies for aminoglycoside recognition. Thus, whereas complexes are, in most cases, stabilized by a significant number of salt-bridges and polar contacts, the specificity seems to be provided by CH/π stacking interactions involving aromatic residues of the protein/RNA and the ligand pyranose/aminocyclitol rings. Key examples of these contacts have been provided by the recently described X-ray structures of kanamycin/ribostamycin in complex with the resistance enzyme AAC(6′),[4d] the ribosomal A-site RNA[5c] and the HIV DIS kissing-loop complex[5e] (Figures 1 and S1). Thus, in the former case, two different tryptophan side-chains participate in contacts with aminoglycoside rings I/II (the numbering used along the manuscript for the different aminoglycoside units and positions is shown in Figure 1). In a similar way, the aminoglucose ring I stacks on a highly conserved guanine ring in both RNA complexes.

Carbohydrate/aromatic CH/π stacking interactions have been shown to play key roles in the recognition of neutral oligosaccharides by proteins.[9−11] They stabilize the complexes by promoting the desolvation of the sugar hydrophobic patches. Additional favorable contributions arise from the interaction between the polarized pyranose CH groups and the aromatic electron density. Moreover, these contacts are extremely sensitive to the axial/equatorial orientation of the different pyranose OH groups and, as a result, they increase the specificity of the binding process.

(6) (a) Zhao, F.; Zhao, Q.; Blount, K. F.; Han, Q.; Tor, Y.; Hermann, T. *Angew. Chem., Int. Ed.* **2005**, *44*, 5329–5334. (b) Blount, K. G.; Zhao, F.; Hermann, T.; Tor, Y. *J. Am. Chem. Soc.* **2005**, *127*, 9818–9829. (c) Revuelta, J.; Vacas, T.; Corzana, F.; Gonzalez, C.; Bastida, A.; Asensio, J. L. *Chem.—Eur. J.* **2010**, *10*, 2986–2991. (d) Francois, B.; Szychowski, J.; Sekhar, S.; Pachamuthu, A. K.; Swayze, E. E.; Griffey, R. H.; Migawa, M. T.; Westhof, E.; Hanessian, S. *Angew. Chem., Int. Ed.* **2004**, *43*, 6735–6738. (e) Nudelman, I.; Rebibo-Sabbah, A.; Cherniavsky, M.; Belakhov, V.; Hainrichson, M.; Chen, F.; Schacht, J.; Pilch, D. S.; Ben-Yosef, T.; Baasov, T. *J. Med. Chem.* **2009**, *52*, 2836–2845. (f) Pokrovskaya, V.; Belakhov, V.; Hainrichson, M.; Yaron, S.; Baasov, T. *J. Med. Chem.* **2009**, *52*, 2243–2254. (g) Luedtke, N. W.; Baker, T. J.; Goodman, M.; Tor, Y. *J. Am. Chem. Soc.* **2000**, *122*, 12035–12036.

(7) (a) Boehr, D. D.; Farley, A. R.; Wright, G. D.; Cox, J. R. *Chem. Biol.* **2002**, *9*, 1209–1217. (b) Gao, F.; Yan, X.; Baettig, O. M.; Berghuis, A. M.; Auclair, K. *Angew. Chem., Int. Ed.* **2005**, *44*, 6859–6862. (c) Gao, F.; Yan, X.; Auclair, K. *Chem.—Eur. J.* **2009**, *15*, 2064–2070. (d) Lombs, T.; Begis, G.; Maurice, F.; Turcaud, S.; Lecourt, T.; Dardel, F.; Micouin, L. *ChemBioChem* **2008**, *9*, 1368–1371. (e) Boehr, D. D.; Draker, K.; Koteva, K.; Bains, M.; Hancock, R. E.; Wright, G. D. *Chem. Biol.* **2003**, *10*, 189–196.

(8) (a) Roestamadji, J.; Graspas, I.; Mobashery, S. *J. Am. Chem. Soc.* **1995**, *117*, 11060–11069. (b) Haddad, J.; Vakulenko, S.; Mobashery, S. *J. Am. Chem. Soc.* **1999**, *121*, 11922–11923. (c) Bastida, A.; Hidalgo, A.; Chiara, J. L.; Torrado, M.; Corzana, F.; Cañadillas, J. M.; Groves, P.; García-Junceda, E.; González, C.; Jiménez-Barbero, J.; Asensio, J. L. *J. Am. Chem. Soc.* **2006**, *128*, 100–116. (d) Asensio, J. L.; Hidalgo, A.; Bastida, A.; Torrado, M.; Corzana, F.; Junceda, E. G.; Cañada, J.; Chiara, J. L.; Jiménez-Barbero, J. *J. Am. Chem. Soc.* **2005**, *127*, 8278–8279.

(9) (a) Quiocho, F. A. *Biochem. Soc. Trans.* **1993**, *21*, 442–448. (b) Lemieux, R. U. *Acc. Chem. Res.* **1996**, *29*, 373–380.

(10) (a) Jiménez-Barbero, J.; Asensio, J. L.; Cañada, F. J.; Poveda, A. *Curr. Opin. Struct. Biol.* **1999**, *9*, 549–555. (b) Chávez, M. I.; Andreu, C.; Vidal, P.; Aboitiz, N.; Freire, F.; Groves, P.; Asensio, J. L.; Asensio, G.; Muraki, M.; Cañada, F. J.; Jiménez-Barbero, J. *Chem.—Eur. J.* **2005**, *11*, 7060–7074. (c) Terraneo, G.; Potenza, D.; Canales, A.; Jiménez-Barbero, J.; Baldridge, K. K.; Bernardi, A. *J. Am. Chem. Soc.* **2007**, *129*, 2890–2900. (d) Fernández-Alonso, M. C.; Cañada, F. J.; Jimenez-Barbero, J.; Cuevas, G. *J. Am. Chem. Soc.* **2005**, *127*, 7379–7386. (e) Ramírez-Gualito, K.; Alonso-Ríos, R.; Quiroz-García, B.; Rojas-Aguilar, A.; Díaz, D.; Jiménez-Barbero, J.; Cuevas, G. *J. Am. Chem. Soc.* **2009**, *131*, 18129–18138.

(11) Laughrey, Z. R.; Kiehna, S. E.; Riemen, A. J.; Waters, M. L. *J. Am. Chem. Soc.* **2008**, *130*, 14625–14633.

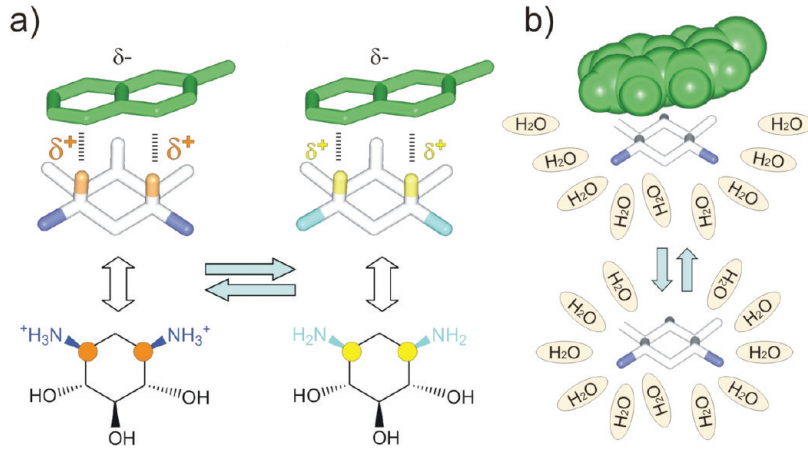

Figure 2. Schematic representation of the different roles that positive charges could play in the stability of the aminoglycoside/aromatic complexes. (a) The polarization of the antibiotic C−H groups is expected to be larger for the protonated ligand. Consequently, an enhancement in the stability of the CH/π bonds would be expected under neutral or acidic conditions. The direct, attractive or repulsive, electrostatic interaction between the different NH_3^+ groups of the drug and the aromatic quadrupole might also have an influence on the complex stability. (b) Aromatic units might affect the solvation of the charged ammonium functions providing a destabilizing contribution at neutral and acid pH values.

Interestingly, little is known about the way densely charged glycosides interact with aromatic rings. In principle, the aminoglycoside polycatonic character could have three differential effects on the stability of the resulting complexes (Figure 2). First, polarization of the pyranose/aminocyclitol CH groups will be more important in the protonated antibiotic, and consequently, CH/π bonds should be pH-sensitive and stronger under neutral or acidic conditions. Second, those ammonium groups located on the stacked sugar/aminocyclitol units could interact electrostatically with the quadrupole of the aromatic ring. Moreover, ammonium groups present on distant sugar units of the aminoglycoside could also be involved in long-range attractive or repulsive NH_3^+/π interactions[12] with the aromatic system. Finally, aromatic units might negatively affect solvation of the charged ammonium functions, providing a destabilizing contribution at neutral and acidic pH values. Indeed, under these particular conditions, the removal of water molecules from the proximity of the antibiotic would have two opposite influences whose net result is unclear; the desolvation of the hydrophobic CH functions, favorable for the formation of the aminoglycoside/aromatic complexes, would be opposed by the unfavorable desolvation of the highly polar -NH_3^+ groups.

Herein, we report a detailed experimental and theoretical analysis of aminoglycoside/aromatic interactions. More specifically, our study aims to determine the influence that the antibiotic polycationic character has on the stability, preferred geometries and internal mobility of the CH/π contacts. With this purpose, the experimental behavior of several aminoglycoside/aromatic interactions has been studied by NMR under a variety of pH and temperature conditions. They varied from simple bimolecular contacts to the more stable intramolecular CH/π bonds present in synthetic derivatives (see below), specifically designed to exhibit different degrees of internal mobility. NMR experiments have been complemented with extensive MD simulations and state of the art ab initio calculations. The obtained results are, in our opinion, of significant relevance for the understanding of the driving forces behind aminoglycoside recognition by RNA or proteins and have clear implications for the design of improved bioactive derivatives.

Results and Discussion

First Evidence for the Unfavorable Influence of the Aminoglycoside Positive Charges on the CH/π Stacking Interactions. NMR Analysis of Simple Bimolecular Complexes. In order to have a first indication of the influence that ammonium groups have on the stability of the aminoglycoside/aromatic complexes, we analyzed by NMR the interaction between natural kanamycin-B (see Figure 1) and benzyl alcohol. This later represents the simplest aromatic system soluble in water and non ionizable in the 1−11 pH range.

The chemical shift perturbations induced in the drug by the presence of this particular aromatic probe were monitored to map out those antibiotic regions involved in specially favored stacking interactions under different pH conditions. A similar methodology has been successfully employed in the analysis of stacking interactions involving neutral monosaccharide units.[10] The results obtained are represented in Figure 3. According to these data, neutral kanamycin-B (pH 10.3) interacts with benzyl alcohol mainly through ring II. Indeed, the axial protons H1-II/H3-II/H5-II (labeled in Figure 3 with red, cyan and yellow circles, respectively) seem to participate in specially favored CH/π bonds with the aromatic probe, as revealed by their negative $\Delta\delta$ values. Significantly, lower chemical shift changes were measured for unit I, whereas for ring III the observed perturbations were almost negligible. This tendency seems to be in agreement with the structural information available for kanamycin-B/RNA or kanamycin-B/protein complexes according to which, aminoglycoside units I/II are clearly preferred to stack on aromatic systems (see Figure 1).[4,5] As a second point, this simple experiment strongly suggests that the aminoglycoside/aromatic interaction is weakened or disrupted by the protonation of the former. Indeed, the chemical shift perturbations detected at pH 10.3 vanish under acidic conditions. Moreover, the remaining minor $\Delta\delta$ values exhibited, in most cases, opposite sign to that expected for a CH/π bond (an upfield shift).

The destabilization of the aminoglycoside/aromatic complexes at low pH values probably reflects the unfavorable influence of

(12) Ma, J. C.; Dougherty, D. A. *Chem. Rev.* **1997**, *97*, 1303–1324.

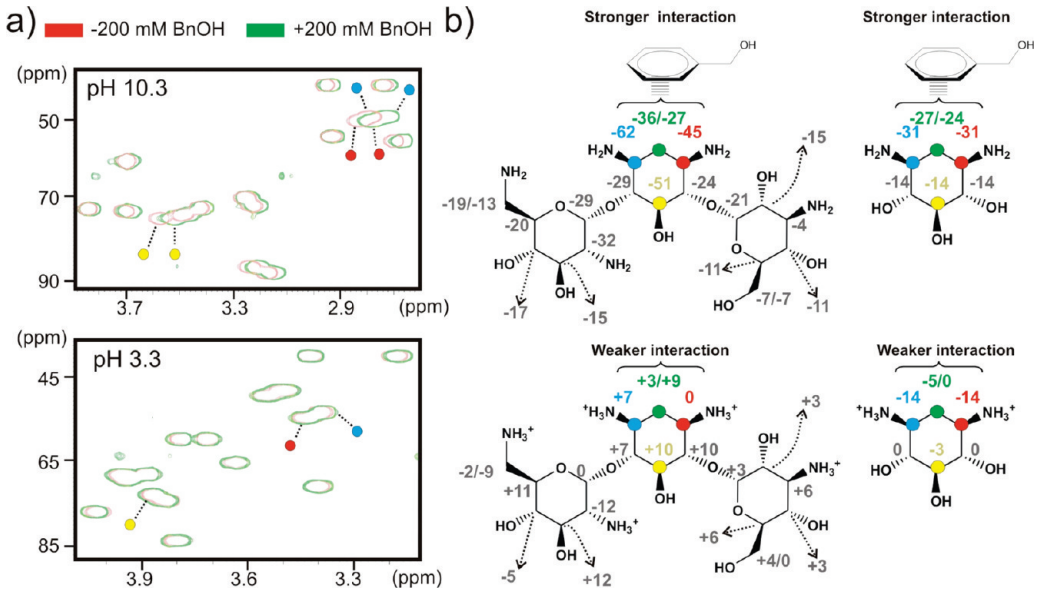

Figure 3. (a) Key regions of HSQC experiments measured at 25 °C for kanamycin-B (20 mM) in the absence (in red) and presence (in green) of 200 mM benzyl alcohol at pH 10.3 (up) and 3.3 (down). Only the outer contour levels are represented for clarity. (b) Proton chemical shift perturbations (ppm/1000) induced at the different positions of kanamycin-B (left) and 2-deoxy-streptamine (right) by the aromatic probe at pH 10.3 (up) and 3.3 (down).

specific NH_3^+ groups. These might include not only those attached to antibiotic units directly involved in CH/π bonds (as the aminocyclitol unit II), but also those located on noninteracting sugar rings. In order to reduce the system complexity, and as a next step, kanamycin-B was replaced by 2-deoxystreptamine (2-DOS). The bimolecular interaction between benzyl alcohol and the aminocyclitol alone was tested employing the same experimental protocol previously described for the complete aminoglycoside. The results obtained are also represented in Figure 3. In this case, minor upfield shifts of particular aminocyclitol signals were detected under acidic conditions. However, as previously observed for kanamycin-B, the $\Delta\delta$ values measured at pH 10.0 are significantly larger than those observed in the fully charged aminocyclitol. In conclusion, aminoglycoside/aromatic complexes seem to be destabilized by the protonation of the antibiotic amino groups. This result might seem surprising considering that the polarization of the drug C−H groups is more important in the fully charged compound. Unfortunately, the labile and presumably highly dynamic character of the previously described bimolecular interactions prevents a precise quantification of the energy penalty imposed by the different NH_3^+ groups.

Design of Kanamycin Derivatives for the Analysis of the Aminoglycoside/Aromatic CH/π Stacking Interactions. The requirement for alternative model systems, able to form more stable aminoglycoside/aromatic complexes, led us to design and synthesize derivatives **1** and **2** (Figures 4 and S2−S3).

Derivative **1** includes a naphthyl ring connected to a α-altrose unit (ring III) by a flexible ethylene linker. The aromatic system is optimally positioned to stabilize hairpin-like structures by means of a stacking interaction with the 2-DOS unit (II). However, transitions between hairpin and disordered conformations would also be feasible. A benzylidene moiety between positions 4 and 6 of the inherently flexible altrose ring (unit III) was incorporated in order to prevent its inversion.

Regarding derivative **2**, its dimeric structure was conceived to promote an intermonomer double stacking between the phenyl rings, and the 2-DOS moieties (units II). Molecular dynamics simulations (MD) demonstrate that these aminocyclitol/aromatic contacts are strongly favored by the aminoglycoside covalent scaffold, so that relatively minor conformational fluctuations around the stacked geometries are allowed (see below). Therefore, **2** provides a stable framework for the analysis of aminocyclitol/aromatic interactions under a variety of pH and temperature conditions.

Considering these general properties, derivative **1** was employed to obtain quantitative information about the influence of the aminoglycoside charges on the stability of the CH/π bonds, whereas **2** was used to asses their effect on the stacking geometry and dynamics.

It should be noted that in both **1** and **2** the aminoglycoside is expected to interact with the aromatic ring through the most favored face of the aminocyclitol unit II. Indeed, these contacts represent the intramolecular version of those between benzyl alcohol and kanamycin-B or 2-deoxystreptamine, previously analyzed (see Figure 3).

As a second consideration, we would like to emphasize that derivatives **1** and **2** were specifically designed to promote the stacking between units II and naphthyl or phenyl rings, respectively. These complexes might exhibit slightly different geometries, which can be broadly classified as parallel-type and nonparallel-type (see Figure 4b), depending on the angle formed by the interacting rings. In the former case, up to 3 axial CH groups of the aminocyclitol moiety (positions H1-II, H3-II, and/or H5-II) could be involved in CH/π bonds with the aromatic system. For nonparallel arrangements, an equatorial position (H2-II) might also participate in such contacts. Both stacking geometries have been well characterized in neutral oligosaccharides.[10] In contrast, those conformations that would allow a direct interaction of the NH_3^+ groups with the aromatic electron density, a pure cation/π bond,[12] are clearly disfavored. Consequently, the influence of the aminoglycoside charges on the stacking could be analyzed without the influence of competing alternative interacting modes.

The synthesis of derivatives **1** and **2** is described in detail in the Supporting Information.

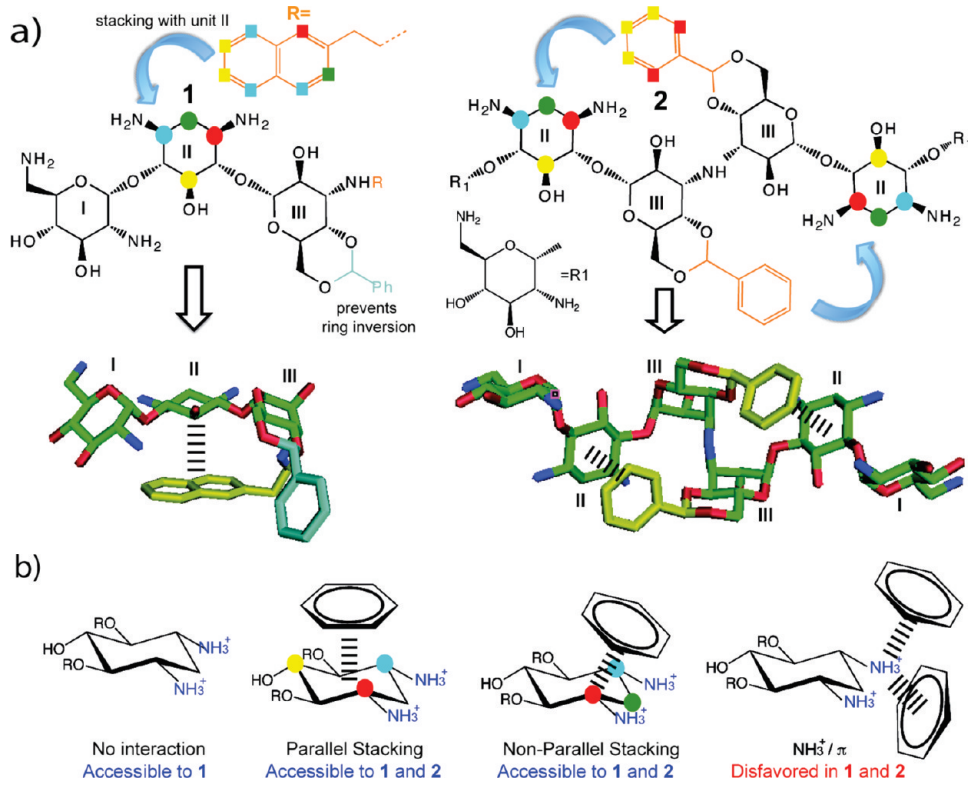

Figure 4. (a) Schematic representation of aminoglycosides **1** (left) and **2** (right) together with the corresponding molecular mechanics minimized models. The stacking interactions between the aminocyclitol unit II and the aromatic rings are highlighted. The colored circles/squares show the code employed to designate the relevant positions of the aminocyclitol and the aromatic system throughout the manuscript. (b) Schematic representation of the different interacting modes between unit II and the corresponding aromatic ring accessible for both **1** and **2**. A maximum of three CH/π contacts are feasible for parallel and nonparallel stacking geometries. The aminocyclitol positions involved are highlighted.

Experimental NMR Analysis of Derivatives 1 and 2 in Solution. Preliminary Experimental Considerations. Our analysis of **1** and **2** involved the measurement of key aminocyclitol/aromatic NOEs and chemical shifts under different pH and temperature conditions. In addition, the pK_a values of the different amino groups were derived from NMR pH-titration experiments. In order to estimate the chemical shift and pK_a perturbations induced in the I/II fragments (see Figure 4) by the aromatic systems ($\Delta\delta$ and ΔpK_a), natural kanamycin-B (represented in Figure 1), together with several natural and synthetic derivatives, all of them including the common neamine core (rings I/II), were employed as reference compounds (Figure S4).

Both $\Delta\delta$ and ΔpK_a values contained relevant information about the aminoglycoside/aromatic complexes. Thus, the chemical shift perturbations measured in **1** provided a first indication of the hairpin population present in solution. In addition, the pattern of $\Delta\delta$ values observed in **1** and **2** was employed to estimate the preferred stacking geometries. This parameter is extremely sensitive to the structural details of the complexes, providing a simple way to identify those aminocyclitol positions involved in preferred CH/π contacts with the aromatic rings (quantum mechanic calculations performed on simple models demonstrate that, in all cases, the corresponding proton signals should be significantly upfield shifted as a result of the interaction, Figure S5).

The pK_a perturbations measured in **1** and **2** provided an estimation of the energy contribution of the different aminoglycoside charges to the stability of the stacked geometries. In our opinion, several experimental aspects of the pK_a analysis deserve special attention. First, the peculiar structure of derivatives **1** and **2** renders the NMR analysis of pK_a values a nontrivial task. The presence of aromatic rings covalently linked to the aminoglycoside scaffold implies that the conformational adjustments that accompany the protonation of the different amino functions may cause significant chemical shift perturbations at distant positions. In order to unambiguously determine pK_a's, all of the ^{1}H and ^{13}C signals were assigned employing 2D-HSQC experiments and their respective changes in chemical shift were monitorized as a function of pH. In addition, heteronuclear $^1J_{CH}$ constants for the HC groups directly attached to amino moieties (HC-NH_2/NH_3^+ fragments) were measured at different pH values. This parameter has been shown to be sensitive to the protonation state of the amino groups, and it is not affected by the ring current effects of aromatic systems.[14]

Second, amino basicities are, to some extent, dependent on the sample conditions. More specifically, salt tends to stabilize the antibiotic protonated form, causing a general increase in the pK_a's.[15] Taking this into account, all of the experiments were performed in absence of added salts. Moreover, to guarantee that the measured pK_a perturbations do not result from minor differences in the sample conditions, the protonation state of **1** and **2** was also checked in the presence of reference aminoglycoside kanamycin-B, employing 1:1 mixtures.

(13) (a) Wang, J.; Li, J.; Cheng, H.; Chang, H.; Tanifum, C. T.; Liu, H.; Czyryca, P. G.; Chang, C. T. *J. Med. Chem.* **2004**, *6*, 1381–1384. (b) Li, J.; Wang, J.; Czyryca, P. G.; Chang, H.; Orsak, T. W.; Evanson, R.; Chang, C. T. *Org. Lett.* **2004**, *6*, 1381–1384.
(14) Freire, F.; Cuesta, I.; Corzana, F.; Revuelta, J.; González, C.; Hricovini, M.; Bastida, A.; Jiménez-Barbero, J.; Asensio, J. L. *Chem. Commun.* **2007**, *2*, 174–176.
(15) Barbieri, C. M.; Pilch, D. S. *Biophys. J.* **2006**, *90*, 1338–1349.

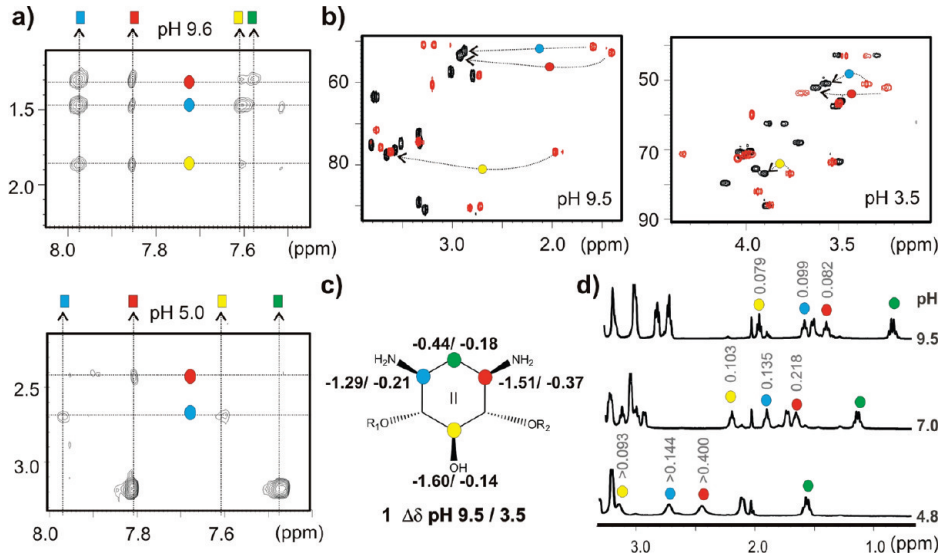

Figure 5. (a) Key region of NOESY spectra collected for derivative **1** at pH 9.6 (up) and 5.0 (down). NOE cross-peaks connecting the naphthyl moiety and the aminocyclitol proton signals are highlighted (color code indicated in Figure 4). (b) A superimposition of HSQC spectra collected for **1** (in red) and kanamycin-B (in black), at basic (left) and acid (right) pH values. (c) Maximum chemical shift perturbations (with respect to kanamycin-B) induced by the naphthyl ring in the aminocyclitol unit at the extreme pH values 9.5 and 3.5. (d) Key region of 1D ^{1}H NMR spectra collected for derivative **1** at pH values 9.5, 7.0, and 4.8 (from top to bottom) and 40 °C. The chemical shifts variations (ppm) measured in the 5−40 °C temperature range are represented above (in gray).

Finally, it should be considered that naphthyl and benzylidene rings present in **1**, confer to this aminoglycoside a certain hydrophobic character and, consequently it was of key importance to rule out its oligomerization/aggregation at the concentration employed in the NMR experiments (0.5 mM). With this objective, control DOSY[16] and dilution experiments were performed under different pH (in the 3−10 range) and temperature (in the 5−40 °C range) conditions. These data unambiguously proved that derivative **1** is monomeric (see Figure S6). Therefore we proceeded with its analysis.

Experimental Analysis of Derivative 1. First, compound **1** was analyzed. NMR data collected at pH >9.0 (the neutral form of the aminoglycoside) confirmed the specific interaction of the naphthyl unit with aminocyclitol ring II. Thus, several cross peaks in NOESY spectra (Figures 5a and S7) demonstrated the proximity between both regions. The presence of a large population of hairpin conformers was further supported by the analysis of the chemical shift perturbations induced by the aromatic ring in the aminoglycoside scaffold (Figures 5b,c and S8). Both, NOE and chemical shift data were consistent with a dominant parallel-type stacking geometry, with three aminocyclitol axial protons (H1−II/H3-II/H5−II) involved in CH/π bonds with the aromatic system. Thus, the most intense NOE contacts (shown in Figure 5a) involved this triad, whose signals were also significantly upfield shifted as a result of the interaction (Figures 5b,c and S8). Indeed, even at 40 °C, chemical shift perturbations measured at this region of **1** were larger than 1 ppm (up to 1.6 ppm for H5). In contrast, the equatorial proton H2-II exhibited only moderate $\Delta\delta$ values and did not present NOE contacts with the naphthyl unit.

The temperature dependence of the ^{1}H NMR spectra provided additional evidence for the stability of the aminoglycoside/aromatic complexes. Thus, it could be observed that, despite their remarkable $\Delta\delta$ values at basic pH, proton signals H1-II/H3-II/H5-II remained sharp even at 5 °C. Moreover, they exhibited small temperature coefficients (Figures 5d and S9). In fact, maximum chemical shift differences in the temperature range 5−40 °C were, in all cases, below 0.1 ppm. Both observations indicate that under these pH conditions, the population of disordered species is very small.

A different behavior was observed at acidic pH values. Thus, at pH 5.0 only extremely weak aminocyclitol/aromatic cross peaks could be detected in NOESY experiments (Figures 5a and S7).

These contacts were absent from the data acquired at pH 3.5 (the fully protonated state of **1**). In addition, under these experimental conditions, chemical shift perturbations at the aminocyclitol moiety were drastically reduced (Figures 5b,c and S8). Finally, in the pH range 4.0−6.0, temperature coefficients of the 2-DOS proton signals were significantly larger than those measured for the neutral aminoglycoside (Figures 5d and S9). Indeed, under these pH conditions, a temperature decrease (from 40 to 5 °C) was accompanied by a significant broadening of the proton signals H1-II, H3-II, and H5-II, reflecting the progressive increase in the hairpin population and the lower exchange rate between hairpin and disordered structures (see Figure S9). An intermediate behavior between those previously described was observed at neutral pH. In conclusion, our analysis demonstrates that, although remarkably stable at pH >9.0, the aminocyclitol/naphthyl stacking is progressively destabilized under neutral and acidic conditions by the protonation of the aminoglycoside.

In order to provide further evidence for the unfavorable influence of the aminoglycoside charges on the stability of the CH/π interactions, pK_a perturbations (ΔpK_a) were determined employing NMR (Figures 6, S10, and S11). Typical titration profiles obtained for **1** at 40 °C are shown in Figure 6a. The pK_a for the amino group at position 2-I was obtained independently from four titration curves (signals C2-I, H2-I, C3-I, and H3-I). To determine the basicity of those amino groups located at ring II, proton and carbon chemical shift changes at positions

(16) Grooves, P.; Rasmussen, M. O.; Molero, M. D.; Samain, E.; Cañada, F. J.; Driguez, H.; Jiménez-Barbero, J. *Glycobiology* **2004**, *14*, 451–456.

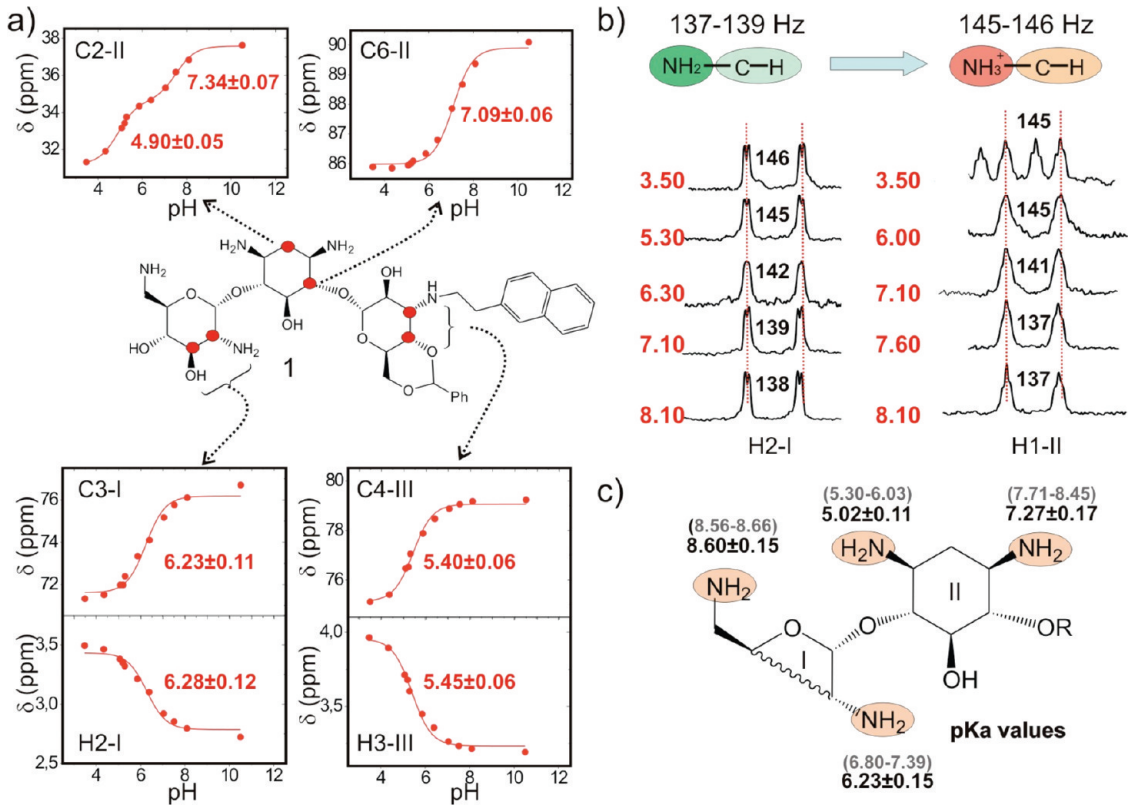

Figure 6. (a) Typical NMR titration profiles obtained for **1** at 40 °C. The monitorized $^{1}H/^{13}C$ signals are indicated. (b) Heteronuclear $^{1}J_{CH}$ constants measured in **1** for the HC-NH_2/NH_3^+ fragments located at positions 2-I and 1-II, under different pH conditions. The information provided by these values was fully consistent with that derived from the chemical shift changes. (c) pK_a values at 40 °C for the amino groups of neamine fragment I/II in **1** (in black) and several related aminoglycosides (including kanamycin-B, see Figures S11 and S14) employed as reference. For these later derivatives, pK_a ranges (in gray), reflecting the variation in the measured basicities, are represented.

2-II and 6-II (highlighted with a red circle in Figure 6a) were monitored. These sites are relatively unaffected by the proximity of the naphthyl system. For position 2-II, two different transitions were apparent, reflecting the sequential change in the protonation state of the amino groups 1-II and 3-II. Therefore, the corresponding pK_a values could be determined independently from a single titration profile. In addition to chemical shifts, heteronuclear $^{1}J_{CH}$ constants were also measured for all the HC-NH_2/NH_3^+ fragments present in the aminoglycoside at different pH values (Figure 6b). The obtained results confirmed the destabilizing influence of the aminoglycoside positive charges. According to the pK_a data, three specific $-NH_3^+$ groups of **1**, those at positions 2-I, 1-II, and 3-II, oppose the aminocyclitol/phenyl stacking interaction. The total pK_a differences with respect to the reference compounds (Figure 6c) amounted, at least, to 1.3 units, which implies that ammonium groups destabilize the stacking interaction by more than 1.9 kcal/mol. This result is fully consistent with the conformational behavior previously described.

Experimental Analysis of Derivative 2. As a next step, the conformational properties of **2** in solution were carefully analyzed. Its structure was designed to strongly favor the aminocyclitol/phenyl interaction, providing a more stable model system for the analysis of CH/π contacts. In agreement with these expectations, the NMR data proved the presence of the predicted intermonomer double stacking under all the pH conditions tested. Thus, clear NOE cross peaks connecting the phenyl ring with the 2-DOS unit were apparent at both, basic and acid pH values (Figure 7a). In addition, significant chemical shifts perturbations (up to −1.8 ppm, Figures 7b and S12) were detected for the aminoclyclitol protons in both, neutral and protonated **2**. Interestingly, the pattern of $\Delta\delta$ values observed under different pH conditions confirmed that aminoglycoside protonation/deprotonation is accompanied by subtle adjustments of the aminocyclitol/phenyl complex. Thus, at pH 9.6 axial protons H1-II, H3-II, and H5-II, were the most affected (see Figure 7b), which is consistent with their participation in CH-π contacts with the aromatic system. This particular interaction mode requires a nearly coplanar disposition of the phenyl and aminocyclitol rings (parallel-type). In contrast, under acidic conditions, the $\Delta\delta$ value for position 5-II was basically maintained, whereas those corresponding to axial H1-II and H3-II and equatorial H2-II proton signals increased, suggesting that, to some extent, this triad was also involved in contacts with the benzylidene moiety (nonparallel complex). Particularly significant is the remarkable upfield shifting measured for the proton signal H1-II at pH 3.5. Overall, the chemical shift perturbations observed in unit II are consistent with a dynamic exchange between different parallel and nonparallel stacking modes (described in Figure 4b), with the first type being predominant at basic pH values and the later under acidic conditions. Moreover, the aminoglycoside protonation promotes a slight shifting of the aromatic system toward the aminocyclitol position H1-II, which seems to participate in especially persistent CH/π contacts (both conclusions were fully supported by the theoretical $\Delta\delta$ values calculated from MD trajectories in solution, see below). Finally, the increased magnitude of the

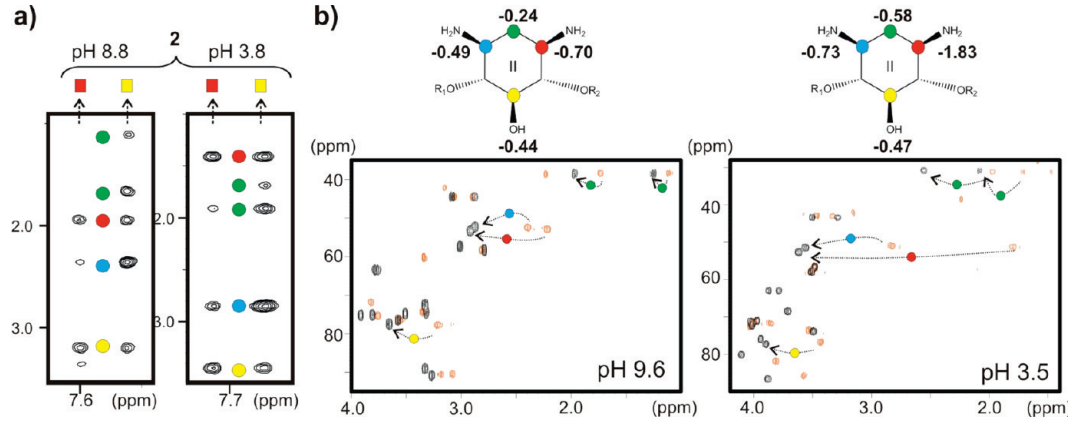

Figure 7. (a) Key region of NOESY spectra collected at pH values 8.8 (left) and 3.8 (right) and 5 °C for derivative **2**. NOE cross-peaks connecting the phenyl moiety and the aminoglycoside proton signals H1-II (red circle), H2-II (green circle), H3-II (cyan circle), and H5-II (yellow circle) are highlighted. (b) Maximum chemical shift perturbations with respect to kanamycin-B, induced in the aminocyclitol unit at 40 °C and the extreme pH values 9.6 (left) and 3.5 (right). A superimposition of HSQC spectra collected for **2** (in red) and kanamycin-B (in black), at acid and basic pH values is also represented.

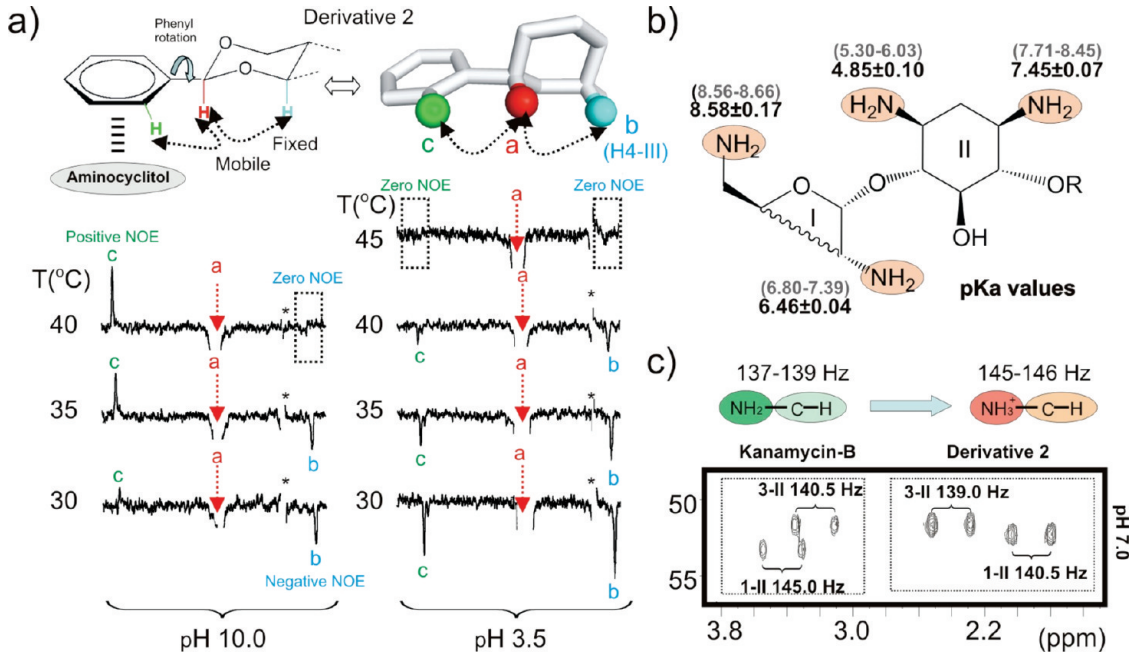

Figure 8. (a) Temperature dependence exhibited by the selective NOEs measured in **2** upon inversion of the benzylidene protons **a** (in red), under basic (left) and acidic (right) conditions. Contacts with protons **b** (in cyan) and **c** (in green) are represented. (b) pK_a values for the amino groups located in neamine I/II fragment of **2** (in black) and several related aminoglycosides (including kanamycin-B, see Figures S13 and S14) at 40 °C. For the reference compounds, a range (in gray), reflecting the variation in measured basicities is represented. (c) Key region of coupled HSQC spectra, acquired for a derivative **2**:kanamycin-B 1:1 mixture at pH 7.0 and 40 °C. The heteronuclear $^1J_{CH}$ constants measured for the HC-NH_2/NH_3^+ fragments located at positions 1-II and 3-II in both, **2** and kanamycin-B, are shown. This parameter is sensitive to the protonation state of the amino groups (as indicated in the upper panel) and demonstrates that, under identical conditions, the amino group 1-II in derivative **2** exhibits a reduced pK_a.

chemical shift perturbations measured at pH 3.5 is also suggestive of a less dynamic aminocyclitol/phenyl interaction.

The apparent decrease in the complex internal mobility at low pH values might reflect the presence of stronger attractive electrostatic forces between the phenyl system and the charged aminocyclitol. Considering the potential relevance of this finding, we looked for additional experimental evidence for the stiffening of the complex under acidic conditions. In principle, this could also be reflected in the rotation rate of the phenyl rings. It should be noted that this conformational transition implies the transient disruption of the aminocyclitol/phenyl CH/π contacts and, consequently, should be specially affected by an enhancement of the electrostatic interactions occurring between both entities. To test this point, we performed selective NOE experiments at different temperatures. Our analysis was focused on two specific contacts, schematically represented in Figure 8a. The benzylidene and altrose protons, **Ha** and **Hb** (also referred as H4-III), are located at a fixed distance (2.4 Å). In contrast, that between **Ha** and phenyl protons **Hc**, should be affected by the internal motion of the aromatic system. Figure 8a shows the temperature dependence exhibited by **Ha/Hb** and **Ha/Hc** NOEs under basic and acidic conditions. It can be observed that at pH 10.0 and 30 °C **Ha/Hb** contact is negative while that between **Ha** and **Hc** almost undetectable. Interestingly, at 35 °C the former NOE remains negative while the later exhibits a clear positive sign. Finally, at 40 °C the **Ha/Hb** contact was basically zero. Overall, these data demonstrate that the **Ha/Hc** pair exhibits a shorter correlation time (and consequently, larger mobility) reflecting the internal motions of the phenyl system. In conclusion, the experimental data

measured for neutral **2** fully supported the dynamic character of the phenyl/aminocyclitol interaction.

A different behavior was observed at low pH values. Indeed, under these conditions **Ha/Hb** and **Ha/Hc** contacts were both negative in the 30−40 °C range. Moreover, both NOEs become zero at the same temperature, around 45 °C (larger temperatures could not be reached with the employed cryoprobe). According to these data, the effective correlation time for both proton pairs are similar, implying that the rotation of the phenyl rings is significantly frozen by the protonation of the aminocyclitol units. This conclusion is in agreement with the chemical shift perturbations observed in charged and neutral **2** and also with the results of the theoretical analysis described in the following sections (see below).

Despite the reduced internal mobility deduced for the aminocyclitol/phenyl complexes under acidic conditions, the analysis of the pK_a perturbations promoted by the aromatic ring demonstrates that aminoglycoside charges are essentially destabilizing (Figures 8b, S13, and S14). The pK_a for the amino group at position 2-I was derived independently from the analysis of four experimental curves (corresponding to C2-I, H2-I, C3-I, and H3-I signals). To determine the basicity of those aminos located on the aminocyclitol ring II, we focused our attention on positions 2-II and 6-II, not involved in CH/π contacts with the phenyl ring.

As previously observed for **1**, three specific NH_3^+ groups of **2** (those at positions 2-I, 1-II, and 3-II) oppose the aminocyclitol/phenyl stacking interaction. Indeed, these moieties exhibited a significantly reduced basicity (out of the range observed for the reference compounds, see Figures 8b,c and S14). Even the amino function 1-II, directly attached to the aminocyclitol position involved in tighter CH/π contacts with the aromatic system (as judged by its large $\Delta\delta$ value), presents a reduced pK_a. This conclusion was further confirmed by the heteronuclear $^1J_{CH}$ constants measured in derivative **2**:kanamycin-B mixtures (see Figure 8c). The total pK_a differences amounted, at least, to 1.0 units implying that positive charges destabilize the stacking interaction by more than 1.4 kcal/mol. In this particular case, the influence of ammonium groups is not sufficient to promote the disruption of the aminocyclytol/phenyl contact, strongly favored by the aminoglycoside covalent scaffold.

Theoretical Analysis of Aminoglycoside/Aromatic Interactions: Molecular Dynamics Simulations. Aminoglycoside Charges and Complex Stability: Molecular Dynamic Simulations of Derivative 1. In order to gain insights into the origin of the peculiar behavior exhibited by **1**, 0.1 μs MD simulations were performed with the AMBER 10.0 package,[17] in the presence of explicit TIP3P water,[18] periodic boundary conditions, and Ewald sums for the treatment of long-range electrostatic interactions.[19] These data allowed a detailed analysis of the water content around **1** (first and second solvation shells) in both the hairpin and disordered conformations. Three different protonation states of the aminoglycoside were considered: the fully protonated and unprotonated structures (5 and 0 positive charges, respectively) and that in which only nitrogen on ring III remains neutral (4 positive charges). This later case was included in our analysis to separate the influence of the linker protonation from that of the rest of amino groups on the aminocyclitol/naphthyl stacking interaction. The obtained results were fully consistent with the experimental observations described in the previous section (Figure 9). Thus, for neutral **1**, hairpin conformations were dominant (95% population). Protonation of all the amino functions, except that on ring III (the linker nitrogen), promoted a severe destabilization of the naphthyl/2-DOS stacking interaction, which amounted to $\Delta\Delta G$ = 1.6 kcal/mol.

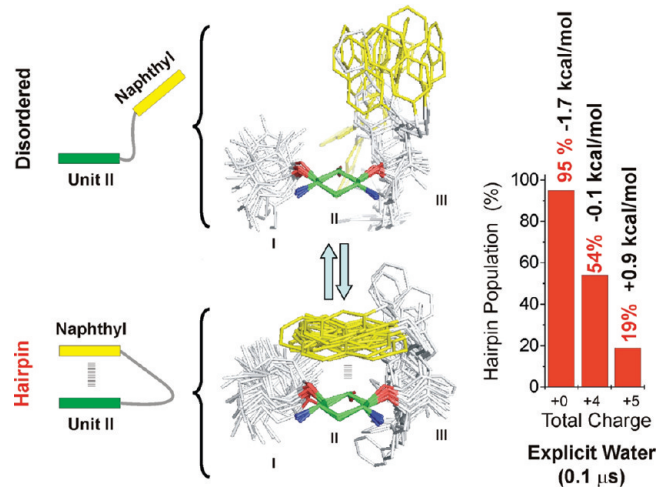

Figure 9. (Left) Ensembles of hairpin (down) and disordered (up) conformers of **1** (total charge +4) obtained from a single 0.1 μs MD simulation performed using explicit TIP3P water. (Right) Population of conformers stabilized by stacking interactions in aminoglycoside **1**, derived from independent 0.1 μs MD trajectories. Three different protonation states were considered: neutral, total charge +4 (neutral linker) and total charge +5. Free energy differences between hairpin and disordered conformers ($\Delta G = G_{hairpin} - G_{disordered}$) estimated from their respective populations are also represented (in black).

Finally, protonation of the whole structure further destabilized the folded state leading to a minor hairpin population (19%).

In order to understand the origin of this effect, we had a thorough look at the solvation of **1** along a selected MD trajectory. More specifically, our analysis was restricted to the system with 4 positive charges (neutral linker). The fluctuations observed in the water content of the aminoglycoside first and second solvation shells are shown in Figure S15a. As expected, transitions from disordered to the more compact hairpin conformations were accompanied by release of water molecules to the bulk. Interestingly, this effect was especially pronounced for the second solvation shell, which, on average, exhibited 15−20 water molecules less for folded structures. We propose that this effect leads to a poorer solvation of the aminoglycoside NH_3^+ functions. In agreement with this hypothesis, the radial pair distribution functions[20] measured for the amino groups 2-I and 1-II showed that hairpin formation promotes an 18−20% reduction in the water content of the second solvation shell (Figure S15b). Intriguingly, for position 3-II a more minor effect was observed. However, it should be considered that the extent of ammonium desolvation might depend critically on the precise geometrical features of the aminocyclitol/naphthyl complexes (see below).

(17) (a) Kollman, P. A.; et al. *AMBER 10*; University of California: San Francisco, 2008. (b) Pearlman, D. A.; Case, D. A.; Caldwell, W. J.; Ross, W. R.; Cheatham, T. E.; DeBolt, S.; Ferguson, D.; Seibel, G.; Kollman, P. *Comput. Phys. Commun.* **1995**, *91*, 1–41.

(18) Mahoney, M. W.; Jorgensen, W. L. *J. Chem. Phys.* **2000**, *112*, 8910–8922.

(19) Darden, T.; Perera, L.; Li, L.; Pedersen, L. *Structure* **1999**, R55–R60.

(20) Corzana, F.; Motawia, M. S.; Hervé du Penhoat, C.; Perez, S.; Tschampel, S. M.; Woods, R. J.; Engelsen, S. B. *J. Comput. Chem.* **2004**, *25*, 573–586.

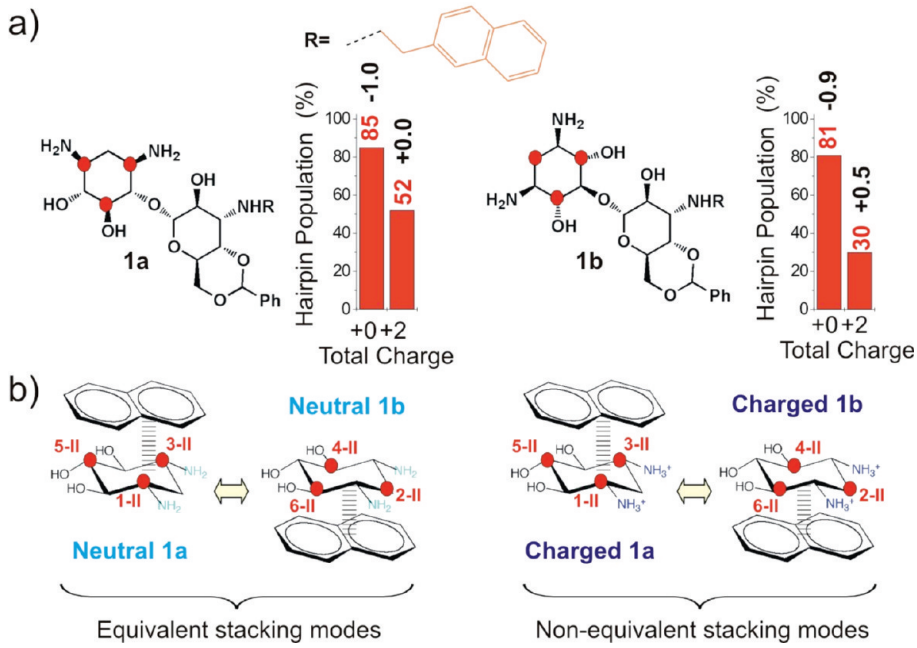

Figure 10. (a) Population of conformers (in red) stabilized by stacking interactions in simpler disaccharide versions of **1** (**1a** and **1b**), estimated from 0.1 μs MD trajectories collected in implicit water. In all cases, two different protonation states were considered: neutral and total charge +2 (linker neutral). Interacting CH groups are highlighted with a red circle. The estimated free energy differences between hairpin and disordered conformers ($\Delta G = G_{\text{hairpin}} - G_{\text{disordered}}$) are indicated in black. (b) The aminocyclitol face involved in CH/π contacts with the naphthyl ring in neutral and charged **1a/1b** is indicated. Equatorial NH_3^+ moieties render both faces of the aminocyclitol unit nonequivalent.

Aminoglycoside Charges and Facial Selectivity: Molecular Dynamic Simulations of Simplified Derivative 1 Models. As a next point, the influence of the positive charges on the facial selectivity of the aminocyclitol/naphthyl interaction was theoretically tested. Previous studies on neutral carbohydrates have shown that stacking complexes are extremely sensitive to the axial/equatorial orientation of the pyranose substituents.[10] More specifically, they seem to be severely destabilized by axial polar groups. In this context, it should be noted that the aminocyclitol unit II, present in **1/2**, includes only equatorial substituents in the most stable ring conformation. Consequently, CH/π contacts established through both faces of this particular ring would be expected to be energetically equivalent. The results previously described for **1** strongly suggest that this hypothesis might be wrong at neutral or acid pH values. Indeed, detailed inspection of minimized models indicates that the charge desolvation penalty associated to both complexation modes could be significantly different. To test this point, 0.1 μs MD trajectories in solution were collected for the simple pseudodisaccharide models, **1a** and **1b**, represented in Figure 10. The former represents a truncated version of derivative **1**. In contrast, model **1b** incorporates an aminocyclitol ring glycosylated at position 5. This alternative pattern of substitution promotes the interaction of the aromatic system with the opposite face of the aminocyclitol unit, which exposes axial protons H2/H4/H6. Consequently, in this model compound, amino groups of ring II are located at positions not directly involved in CH/π bonds. In addition, this particular arrangement would place charged NH_3^+ moieties closer to the aromatic system, which might determine a larger desolvation penalty. For our theoretical analysis, only the neutral state of the models (**1a** and **1b**) and that with the aminocyclitol charged (the linker remains neutral) were considered. On this occasion, the less demanding generalized Born model with the Bashford modification was employed to simulate the water environment.[21]

As expected, for the neutral aminoglycosides the MD trajectories predicted similar hairpin populations. Moreover, in both cases, they were destabilized by the protonation of the aminocyclitol unit. Interestingly, this effect was significantly more pronounced in charged model **1b** (Figure 10). Considering the particular location of the positive charges in this system (at positions not involved in CH/π contacts and far from the altrose ring), the observed effect should reflect, almost exclusively, the higher energy penalty associated to their partial desolvation. In conclusion, the presence of equatorial NH_3^+ moieties renders both faces of the aminocyclitol unit nonequivalent. This example illustrates how charged groups can contribute to increase the specificity of the antibiotic/aromatic complexes, favoring discrimination between otherwise equivalent stacking arrangements.

Influence of the Aminoglycoside Charges on the Stacking Geometry and Dynamics: Molecular Dynamic Simulations of Derivative 2. To test the influence of the aminoglycoside charges on the preferred geometry and dynamics of the aminocyclitol/aromatic complexes, we performed MD simulations with derivative **2**, employing implicit water.[21] First, two different protonation states of **2** were considered. They included the neutral form, and that with rings I and II fully charged (total charge +8). Given that, in this particular case, the aminoglycoside covalent scaffold should allow only relatively minor conformational fluctuations, simulation lengths were limited to 20 ns. The obtained results are represented in Figure 11. It can be observed that, in all cases, stacking interactions between the 2-DOS and the phenyl rings were maintained during the whole trajectories. Interestingly, their precise geometries varied depending on the aminoglycoside charge. Thus, for the neutral molecule, the phenyl unit adopted mainly a parallel arrangement,

(21) Onufriev, A.; Bashford, D.; Case, D. A. *Proteins* **2004**, *55*, 383–394.

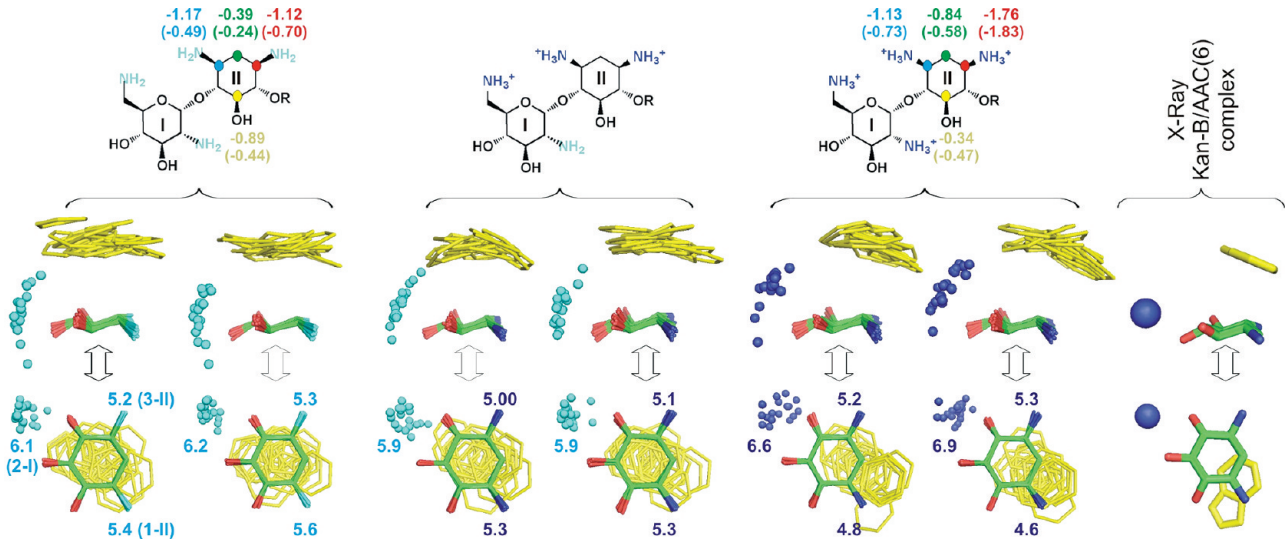

Figure 11. Conformational ensembles obtained from 20 ns MD simulations of **2** in solution. The aminocyclitol and phenyl moieties are represented with sticks and the nitrogen atoms at position 2-I with spheres. Other regions of the molecule are omitted for clarity. Two different views related by a 90° rotation around the *x* axis are shown. Three different protonation states of the dimer were considered; (from left to right) neutral, only positions 6-I/1-II/3-II charged and finally, rings I/II charged. Protonated and neutral amino groups are shown in blue and cyan, respectively. Average chemical shift perturbations ($\Delta\delta$) at key positions of the aminocyclitol unit calculated from the MD ensembles are represented on the top together with experimental NMR values (in brackets). In addition, average distances between nitrogen atoms 2-I, 1-II, and 2-II and the geometrical center of the phenyl rings are represented in the lower panels (also in blue or cyan). Finally, the experimental stacking geometry observed in the kanamycin-B/AAC(6′) complex according to X-ray studies (pdb code 2QIR) is shown in the right panel for comparison.

in which the aminocyclitol ring interacts with the aromatic system through axial protons H1-II/H3-II/H5-II. In contrast, in protonated **2**, the aromatic system was clearly displaced toward position 1-II, fluctuating between parallel and nonparallel stacking modes. This conformational rearrangement implies that the aminocyclitol equatorial proton H2-II was transiently involved in CH/π contacts with the aromatic system. In order to validate the MD simulations, chemical shift perturbations at key aminocyclitol positions H2-I/H1-II/H3-II/H5-II, in neutral and protonated **2**, were theoretically evaluated from the corresponding conformational ensembles and compared with the experimental values.

It should be noted that this represents a demanding test, given the extreme sensitivity of the $\Delta\delta$ values to minor structural variations and the dynamic character of the aminocyclitol/phenyl complex. As shown in Figure 11, the variations in $\Delta\delta$ with the pH deduced from the simulations were in a reasonable agreement with the experimental trends. More specifically, the MD data correctly reproduced the remarkable increase in $\Delta\delta$ for the aminocyclitol position H1-II detected at low pH. Also in agreement with the experimental observations, the theoretical $\Delta\delta$ value for the equatorial position H2-II was significantly increased in charged **2**. Both $\Delta\delta$ changes are consistent with a larger population of nonparallel complexes under acidic conditions.

To gain insights into the origin of this effect, the distances from the phenyl rings to the NH_2/NH_3^+ groups located at the key positions 2-I, 1-II, and 3-II were monitorized along the MD trajectories (Figure 11). It can be observed that the subtle conformational change, induced by the protonation of rings I/II, places the aromatic systems closer to the aminocyclitol ammonium group 1-II, whereas its average distance to the ammonium group 2-I is increased. A simple explanation for this behavior is that the position of the phenyl rings in the charged aminoglycoside is carefully adjusted to globally minimize unfavorable contacts with the surrounding NH_3^+ functions. In this particular case, the improvement in the solvation of position 2-I promoted by the conformational change might overcompensate the more pronounced desolvation of the aminocyclitol charged functions. In order to theoretically test this hypothesis, we considered a different protonation state of dimer **2**. Starting from the previously analyzed charged derivative, NH_3^+ groups at key positions 2-I were selectively neutralized (rendering a total charge +6) and a third 20 ns MD trajectory was collected. As shown in Figure 11 (middle panels), this single modification had a large effect on the aminocyclitol/phenyl stacking. It can be observed that, on this occasion, the obtained conformational distribution was quite similar to that predicted for the neutral system. This result supports the conclusion that NH_3^+ at position 2-I has a significant influence on the stacking geometry. Interestingly, the precise geometrical features of the aminocyclitol/aromatic interaction deduced for protonated **2**, closely resemble those observed in the kanamycin-B/AAC(6′) complex, recently described by X-ray methods (see Figure 11, right panel), suggesting that similar NH_3^+/aromatic interactions might determine the preferred stacking arrangement in natural systems.[4d]

As a second point, according to the MD simulations, the dynamic character of the aminoglycoside/aromatic stacking interaction is significantly reduced upon protonation of the aminocyclitol unit. The stiffening of the structure is mainly illustrated by the reduced rotation rate exhibited by the two aromatic moieties. Thus, for neutral **2**, several transitions, consisting in a 180° rotation of the phenyl ring (to generate equivalent stacking modes), were observed. It should be noted that these conformational changes require the transient disruption of the CH/π contacts. In contrast, only few transitions were apparent in the MD simulations collected with ring II being protonated (Figure S16). This behavior is fully consistent with the experimental NMR analysis of **2** previously described (see the quantum mechanics analysis of simple models described in the following sections for a detailed explanation of this effect).

Two conclusions can be derived from this analysis:

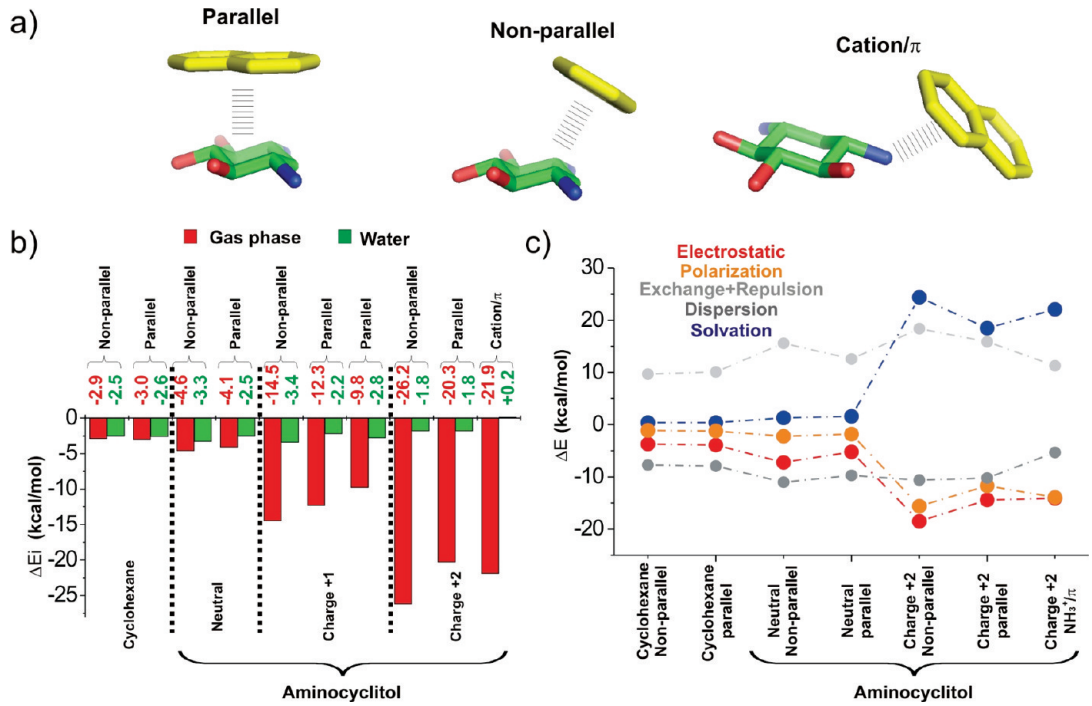

Figure 12. (a) Quantum mechanics optimized structures for aminocyclitol(protonated form)/naphthalene pair in the different interaction geometries considered. (b) Counterpoise-corrected interaction energies, related to the sum of isolated monomers, calculated at the SCS-MP2/6-311G(2d,p)//PCM/M06−2X/TZVP level in the gas phase (red) and water (C-PCM-corrected values, in green). Different protonation states of the aminocyclitol moiety were considered. Interaction energies derived for the analogous cyclohexane/naphthalene complexes are also shown for comparison. (c) Diverse contributions (electrostatic, polarization, exchange, repulsion, and dispersion) to the interaction energies calculated through the localized molecular orbital energy decomposition analysis (LMO-EDA) are schematically represented. Noteworthy, attractive dispersion forces are the responsible for the stacking interactions for cyclohexane and neutral aminocyclitol. Any attempt to locate stacked geometries employing methods in which dispersion forces are poorly considered (i.e. B3LYP) failed.

First, the precise geometrical features of the aminocyclitol/aromatic stacking seem to result from a delicate balance between different NH_3^+/aromatic interactions involving not only the aminocyclitol charges but also those located in the vicinal sugar units. This observation has implications for the molecular recognition of aminoglycosides by protein or RNA receptors. Most antibiotics of this family include a variable number of positive charges, in the 4−6 range, at physiological pH. By minimizing unfavorable contacts with specific aromatic functions of the receptor, the antibiotic NH_3^+ groups might determine a unique binding mode contributing to the specificity of the recognition process.

Second, despite their globally destabilizing influence, aminoglycoside charges reduce de dynamic character of the CH/π complexes probably reflecting an enhancement in the electrostatic interactions occurring between the aromatic and the aminosugar/aminocyclitol rings.

Theoretical Analysis of Aminoglycoside/Aromatic Interactions: Quantum Mechanics Calculations. Aminoglycoside Charges and Complex Stability: Quantum Mechanics Calculations of Simplified Derivative 1 Models. To further understand the theoretical basis of the observed behavior, quantum mechanics (QM) calculations were performed on a very simple version of derivative **1**, an isolated aminocyclitol/naphthalene pair. The neutral, intermediate (charge +1), and fully protonated (charge +2) states of the aminocyclitol were considered. Several stacked structures were located and energy-minimized. They comprised both parallel and non-parallel geometries showing clear CH/π interactions. In addition, a distorted T-shaped arrangement biased by NH_3^+/π interactions (only for the fully charged model) was also considered. The aminocyclitol/naphthalene interaction energies were derived at the SCS-MP2/6-311G(2d,p) level on the energy-minimized geometries calculated at the PCM/M06-2X/TZVP level.[23,24] Bulk solvent effects were considered implicitly through different variants of the polarizable continuum model for both geometry optimizations (IEF-PCM[25] as implemented in Gaussian 09) and single-point energy calculations (C-PCM[26] as implemented in Gamess). For comparison purposes, the analogous cyclohexane/naphthalene complexes were also evaluated employing the same theoretical protocol.

The counterpoise-corrected interaction energies obtained are represented in Figure 12. As can be seen through these data, neutral aminocyclitol/naphthalene complexes are stabilized by 4.1/4.6 kcal/mol in the gas phase (ΔEi_{gas}), depending on the particular geometry considered. It can be observed that the ΔEi_{gas} values derived for the protonated models (charge +1 and +2) are much more favorable than those corresponding to the neutral pairs, which is likely due to the enhancement of the CH/π interactions by the presence of ammonium groups. While attractive dispersion forces are of similar magnitude in all cases,

(22) Frisch, M. J.; et al. *Gaussian 09*, revision A.2; Gaussian, Inc.: Wallingford, CT, 2009.
(23) Zhao, Y.; Truhlar, D. G. *Theor. Chem. Acc.* **2008**, *120*, 215–241.
(24) (a) Schaefer, A.; Horn, H.; Ahlrichs, R. *J. Chem. Phys.* **1992**, *97*, 2571–2577. (b) Schaefer, A.; Huber, C.; Ahlrichs, R. *J. Chem. Phys.* **1994**, *100*, 5829–5835.
(25) (a) Cossi, M.; Barone, V.; Mennucci, B.; Tomasi, J. *Chem. Phys. Lett.* **1998**, *286*, 253–260. (b) Tomasi, J.; Mennucci, B.; Cancés, E. *J. Mol. Struct.* **1999**, *464*, 211–226. (c) Cossi, M.; Scalmani, G.; Rega, N.; Barone, V. *J. Chem. Phys.* **2002**, *117*, 43–54. (d) Tomasi, J.; Mennucci, B.; Cammi, R. *Chem. Rev.* **2005**, *105*, 2999–3093.
(26) (a) Barone, V.; Cossi, M. *J. Phys. Chem. A* **1998**, *102*, 1995–2001. (b) Cossi, M.; Rega, N.; Scalmani, G.; Barone, V. *J. Comput. Chem.* **2003**, *24*, 669–681.

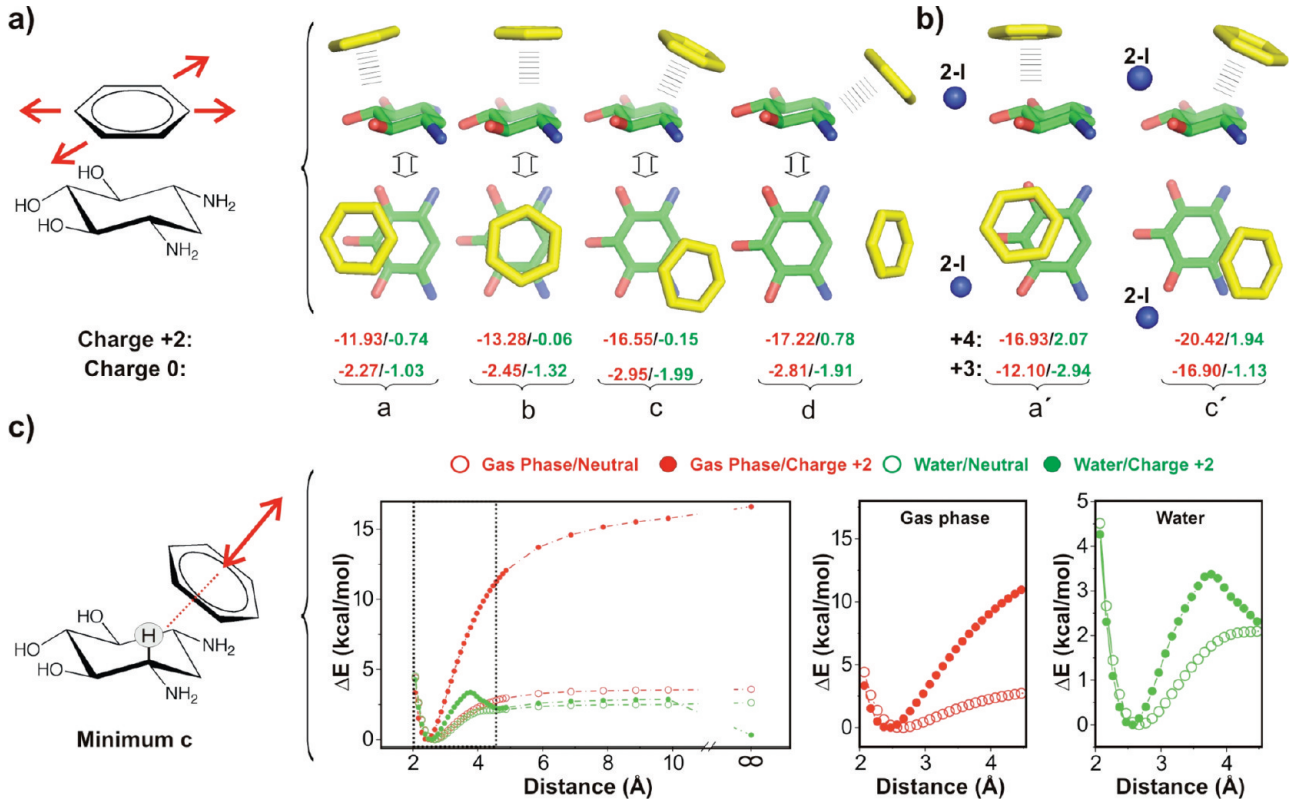

Figure 13. (a) Quantum Mechanics optimized structures for an aminocyclitol (protonated form)/benzene pair in the different interaction geometries considered (labeled as **a**−**d**). Counterpoise-corrected interaction energies, related to the sum of isolated monomers, calculated for the fully charged and neutral complexes, at the SCS-MP2/6-311G(2d,p)//PCM/M06-2X/TZVP level, both in gas phase (red) and water (C-PCM-corrected values, in green) are shown. Geometry **b** corresponds to a transition state. (b) Quantum mechanics optimized structures for the pseudodisaccharide fragment I/II in complex with a simple aromatic ring (toluene). The aromatic and aminocyclitol moieties are represented with sticks while the amino function at position 2-I is represented with a sphere. Two different protonation states of the system were considered (total charge +3 and +4, see the main text). Interaction energies in the gas phase and in water are shown in red and green, respectively. (c) BSSE-corrected dissociation potentials for a neutral and charged aminocyclitol/phenyl complex (minimum **c**), calculated at the SCS-MP2/6-311G(2d,p) level, both in the gas phase (red curves) and in solution (C-PCM, green curves). Expansions of the curves (2−4.5 Å) in the gas phase and in water are shown on the right.

the observed extra stabilization of the stacked geometries could be related, hence, to greater long-range electrostatic and induction (polarization) interactions occurring between the dipole moment of the aminocyclitol and the quadrupole moment of naphthalene. This view is supported by an analysis of the diverse contributions to the interaction energies, calculated through the localized molecular orbital energy decomposition analysis, LMO-EDA[27] (Figure 12c). Strikingly, this scenario is completely inverted when bulk solvation effects are taken into account. Thus, the enhanced interaction energies derived in the gas phase for the protonated complexes are overcompensated by significantly less favorable solvation energies with respect to the isolated molecules.

Overall, full protonation of the aminocyclitol ring is predicted to destabilize the stacked geometries by 0.7−1.5 kcal/mol, which is in good agreement with the experimental analysis previously described. It should be mentioned that, according to these calculations, the unfavorable influence of ammonium desolvation is more pronounced for a pure NH_3^+/π interaction. This might explain why, in contrast to stacking interactions, such contacts are highly infrequent in protein/aminoglycoside or RNA/aminoglycoside complexes. In agreement with this idea, a recently reported study shows that the influence of direct NH_3^+/π bonds on the stability of a specific protein/ligand complex is negligible, which was attributed to the energy penalty associated to ammonium desolvation.[28]

Influence of the Aminoglycoside Charges on the Stacking Geometry and Dynamics: Quantum Mechanics Calculations of Simple Derivative 2 Models. As a next step, the influence of the aminocyclitol charges on the stacking geometry was analyzed. Because of the reduced size of the aromatic moiety (benzene) with respect to the naphthalene system, the localized minima, represented in Figure 13, were somewhat different to those previously described. Thus, a number of parallel and nonparallel stacked geometries, with one to two axial protons of the aminocyclitol involved in CH/π bonds with the aromatic ring, were found and characterized as local minima at the PCM/M06−2X/TZVP level (labeled as **a**, **c**, and **d** in Figure 13). In contrast, parallel arrangements with three interacting aminocyclitol axial CH positions, were characterized as local transition states in the corresponding potential energy surface (**b**). This observation is in agreement with previous results reported for carbohydrate-phenyl interactions in neutral systems.[10] The corresponding counterpoise-corrected aminocyclitol/phenyl interaction energies, both in the gas phase and in water, are also represented in Figure 13. Regarding the neutral system, it can be observed that nonparallel arrangements (**c** and **d**) are always

(27) Su, P.; Li, H. *J. Chem. Phys.* **2009**, *131*, 1–15.

(28) Salonen, L. M.; Bucher, C.; Banner, D. W.; Haap, W.; Mary, J.-L.; Benz, J.; Kuster, O.; Seiler, P.; Schweizer, W. B.; Diederich, F. *Angew. Chem., Int. Ed.* **2009**, *48*, 811–814.

slightly favored. Interestingly, protonation of the aminocyclitol ring has a remarkable influence, not only on the complex stability but also on its preferred geometry. In the gas phase, both properties seem to be determined by attractive electrostatic interactions between the aromatic system and the charged aminocyclitol ring. In contrast, the energy cost associated to NH_3^+ desolvation is the dominant effect, when water is implicitly considered. In agreement with this view, nonparallel arrangements (**c** and **d**), which place the phenyl ring closer to the charged NH_3^+ functions, are clearly preferred in the gas phase. In water, these stacking modes are more severely destabilized by the charge desolvation penalty, leading to a complete reversal in the geometrical preferences of the aminocyclitol/phenyl complex. Indeed, arrangement **a**, which place the aromatic ring further from the NH_3^+ groups, represents the most stable minima in aqueous solution. It should be noted that both, in the gas phase and in water, energy differences between the alternative stacking modes considered are larger for the charged system, which implies that the protonation of the aminocyclitol ring enhances the specificity of the complex.

The analysis previously described allowed an identification of the preferred arrangements for isolated aminocyclitol/benzene pairs. However, in the context of a complete aminoglycoside, NH_3^+ groups located in vicinal sugar units could also modulate the stacking. Indeed, both, the experimental NMR data and the MD trajectories collected for **2**, indicate that position 2-I of this derivative has a remarkable influence on the complex geometry. In order to test this particular point, we also analyzed the interaction of the (more realistic) complete pseudodisaccharide I/II fragment with a toluene molecule. Minimum energy geometries for the complexes, together with the corresponding interaction energies in the gas phase and in water, were derived considering two different protonation states of the model: that with rings I/II fully charged (total charge +4) and that with position 2-I selectively neutralized (total charge +3). The results obtained are represented in Figure 13b. According to these data, the fully protonated minima exhibit enhanced interaction energies (−16.93 vs −12.10 and −20.42 vs −16.90 kcal/mol for geometries **a′** and **c′**, respectively) in the gas phase, implying that long-range NH_3^+/aromatic electrostatic interactions established through the aminoglycoside position 2-I are globally attractive. Moreover, this particular contact has a significant influence on the preferred geometry of the complexes. Thus, while the nonparallel geometry (**c′**) is always favored (reflecting the dominant role of the aminocyclitol/aromatic electrostatic interactions) its relative stability with respect to the parallel arrangement (**a′**) is reduced by 1.31 kcal/mol in the fully charged model.

It can be observed that the former geometry places the aromatic ring further from the NH_3^+ 2-I, leading to a weaker contact.

On the other hand, in water, NH_3^+/aromatic interactions become globally unfavorable, so that position 2-I strongly destabilizes the parallel arrangement **a′**. In contrast with the behavior predicted for the isolated aminocyclitol/phenyl pair (see Figure 13a), now the nonparallel geometry (minimum **c**), with the aromatic ring proximate to the aminocyclitol NH_3^+ groups, is preferred. These results are in good agreement with the conclusions of both the NMR and MD analysis of **2** described in previous sections.

As a final point, the influence of aminoglycoside charges on the energy cost for low amplitude fluctuations, implying the transient disruption of CH/π bonds, was tested. With this objective, an arbitrary geometry of a simple aminocyclitol/benzene complex (that of minimum **c**, see Figure 13) was selected and the dissociation potential was evaluated both, in the gas phase and implicit water. Potential energy curves were calculated at the SCS-MP2/6-311G(2d,p) level through nonrelaxed scans of the distance between the H1 hydrogen of the aminocyclitol moiety (both in neutral and protonated states) and the center of the benzene ring. The obtained results are represented in Figure 13c. Two specific features of the obtained profiles deserve special attention. First, in water, formation of the charged complex proceeds through an energy barrier, which can be related to the penalty associated with charge desolvation. On the contrary, these processes are barrierless in the neutral state at this theoretical level. Second, in all cases, the potential energy curve derived for the charged complex exhibits a more pronounced slope in the proximity of the stacked geometry, which represents narrower energy minima. These results might seem surprising considering that in water NH_3^+ solvation opposes CH/π interactions. However, it should be noted that, for low amplitude fluctuations, the empty space generated between the stacked entities might not be solvent accessible so that the disruption of the CH/π bonds cannot be compensated by an improvement in the NH_3^+ solvation. As a result, low amplitude fluctuations of the aromatic ring along this particular reaction coordinate, are significantly hampered by the protonation of the aminocyclitol unit, even in presence of water. This conclusion is in excellent agreement with the reduced rotation rate exhibited by phenyl rings in charged derivative **2**.

To summarize, in the gas phase or low dielectric environments, a delicate balance among different CH/aromatic interactions enhanced by adjacent NH_3^+ groups determines the preferred geometry of the aminoglycoside/aromatic complexes. This scenario is drastically altered when water solvation is taken into account. Under these circumstances, the position of the aromatic ring within the complex seems to be optimized to globally minimize desolvation of the surrounding ammonium functions. Finally, both in the gas phase and water, NH_3^+ functions seem to increase the complex specificity and reduce its dynamic character, as a result of the enhanced electrostatic attraction between the aminocyclitol and the aromatic ring.

Role of Aromatic Rings in the Molecular Recognition of Aminoglycoside Antibiotics: Implications for Drug Design. Finally, some comments regarding the implications of the results described along the manuscript for the molecular recognition of aminoglycoside antibiotics and the design of improved derivatives should be made.

From a molecular recognition perspective, the apparent conflict between the highly polar nature of these antibiotics and the hydrophobic character of the aromatic side-chains frequently found in aminoglycoside receptors is intriguing. Ammonium groups are known to contribute importantly to the stabilization of aminoglycoside complexes with RNA or proteins. Thus, they participate in salt bridges or hydrogen bonds with the receptor polar groups and interact electrostatically with the usually strongly anionic binding pockets. In fact, aminoglycoside binding to RNA/proteins is, in most cases, coupled to the protonation of several amino functions of the ligand.[29] It could be hypothesized that under these circumstances the contribution of stacking interactions to the complex stability might be reduced

(29) (a) Kaul, M.; Barbieri, C. M.; Kerrigan, J. E.; Pilch, D. S. *J. Mol. Biol.* **2003**, *326*, 1373–1387. Kaul, M.; Pilch, D. S. *Biochemistry* **2002**, *41*, 7695–7706.

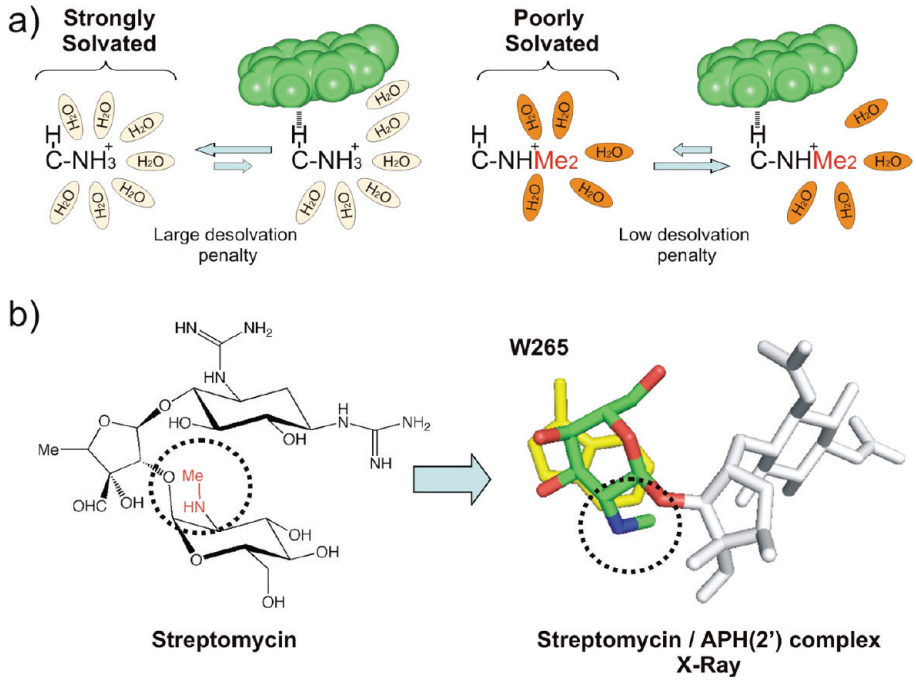

Figure 14. (a) CH/π interactions involving CH−NH_3^+ fragments can be stabilized by the *N*-methylation of the amino groups.[29] The influence of this particular modification on the binding equilibrium is schematically represented. (b) *N*-Methyl groups are present in a minor fraction of naturally occurring aminoglycosides, as streptomycin (shown on the left). The recently described structure of this antibiotic in complex with the resistance enzyme APH(2′) (pdb code 3HAV) reveals a clear interaction between the antibiotic *N*-methylated glucose unit and a tryptophan side-chain.

with respect to that usually observed for neutral oligosaccharides. However, this will largely depend on the extent of ammonium desolvation promoted by the hydrophobic aromatic rings in the complexed state. The desolvation penalty would be expected to be relatively minor for those particular NH_3^+ groups already hidden to solvent by extensive polar contacts with the receptor. In these cases, stacking and polar interactions might operate synergistically to stabilize the complexes (Figure S17). Thus, by neutralizing the positive charge of the ammonium groups and promoting their total desolvation, the NH_3^+/receptor contacts would favor the stacking of the aminoglycoside rings with aromatic systems. In turn, the hydrophobic environment provided by the aromatic residues might cooperatively enhance the strength of the former polar interactions. On the contrary, desolvation of unpaired NH_3^+ groups of the antibiotic by the receptor aromatic side-chains might be significantly unfavorable. However, even in these circumstances stacking CH/π interactions could be essential to discriminate between alternative binding modes, increasing the complex specificity. Indeed, our analysis demonstrates that the ligand charges impose strict requirements on the preferred geometry of the aminoglycoside/aromatic complexes and reduce their dynamic character.

From a medicinal chemistry perspective, the obtained results have interesting implications. Thus, they strongly suggest that aminoglycoside binding to both RNA and protein receptors might be significantly enhanced by the *N*-methylation of specific amino functions (Figure 14a). This modification (originally proposed by Waters et al. for the stabilization of CH/π contacts)[30a] would limit the energy penalty associated to ammonium desolvation, while preserving the intense ligand/receptor electrostatic interactions. Indeed, *N*-methylation has been shown to stabilize lysine/tryptophan interactions in model β-hairpin peptides and specific protein/ligand complexes.[28,30] Despite the evident potential of this strategy within the aminoglycoside field, its scope and limitations have not been explored yet.

Finally, it should be mentioned that, *N*-methyl groups are present in a minor fraction of natural aminoglycosides, as gentamycin, spectinomycin or streptomycin. Interestingly, the recently described X-ray structure of streptomycin in complex with resistance enzyme APH(2′) reveals a unique aminoglycoside/aromatic contact that precisely involves the antibiotic *N*-methylated aminoglucose unit (Figure 14b). Probably, this specific *N*-methyl group plays a significant role in the stabilization of the enzyme/substrate complex.

Conclusions

We have performed a detailed experimental and theoretical analysis of the role played by CH/π stacking interactions in the molecular recognition of polycationic glycosides. With this purpose, different aminoglycoside/aromatic pairs have been selected as model systems. These comprised totally unconstrained bimolecular complexes together with several intramolecular versions of the former, with decreasing degrees of conformational freedom (derivatives **1** and **2**). The results obtained through this study demonstrate that:

(a) Aminoglycoside/aromatic CH/π interactions in the gas phase (and presumably also in low dielectric environments) are significantly enhanced by the protonation of the antibiotic. Favorable electrostatic forces occurring between the drug and the aromatic quadrupole are at the origin of this effect.

(30) (a) Hughes, R. M.; Waters, M. L. *J. Am. Chem. Soc.* **2005**, *127*, 6518–6519. (b) Hughes, R. M.; Waters, M. L. *J. Am. Chem. Soc.* **2006**, *128*, 13586–13591. (c) Tatko, C. D.; Waters, M. L. *J. Am. Chem. Soc.* **2004**, *126*, 2028–2034.

(b) On the contrary, in water, aminoglycoside NH_3^+ groups destabilize the complexes. The energy penalty associated to desolvation of the antibiotic charged functions, promoted by the aromatic systems explains this behavior.

(c) Ammonium groups increase the specificity of the aminoglycoside/aromatic complexes and reduce their internal mobility both, in the gas phase and in water. More specifically, low amplitude fluctuations implying the transient disruption of the CH/π bonds are significantly hampered by the protonation of the antibiotic. The stiffening of the complex reflects the enhancement of the electrostatic interactions between the charged aminosugar/aminocyclitol rings and the aromatic system. This conclusion is in good agreement with results previously reported by Waters et al. for lysine/tryptophan CH/π interactions in model peptides.[30b,c]

(d) Electrostatic forces and charge desolvation are also the dominant factors that determine the facial selectivity and preferred geometry of the aminoglycoside/aromatic complexes, in gas phase and water, respectively.

The results reported herein contribute to the understanding of the driving forces behind aminoglycoside recognition and should be carefully considered in the design of improved aminoglycoside based ligands.

Materials and Methods

The Synthesis of derivatives **1** and **2** together with a detailed characterization of the synthetic intermediates is included in the Supporting Information.

NMR Experiments. NMR experiments were recorded on Bruker Avance 600 and Varian Unitiy 500 spectrometers equipped with cryoprobes at 278−313 K.

The interaction of benzyl alcohol (200 mM) with kanamycin-B (20 mM) and 2-deoxy-streptamine (30 mM) was tested at 25 °C using HSQC experiments. The chemical shift perturbations induced at the different positions of these aminoglycosides by the aromatic probe were monitored at pH 10.3 and 3.3.

Samples of **1** and **2** were prepared in D_2O at 0.1−1.0 mM concentrations and several pH values in the 3.0−10.5 range. Dilution experiments were performed (up to 20 μM) in order to rule out the presence of a significant aggregation of the aminoglycoside under the employed experimental conditions. For derivative **1**, DOSY experiments[16] were also collected under different experimental conditions to prove its monomeric nature (Figure S6).

The ^{1}H and ^{13}C assignments of **1** and **2** were derived from a set of 2D-NOESY, TOCSY and DQF-COSY experiments carried out in the phase-sensitive mode using the TPPI method. For the NOESY experiments, mixing times from 100 to 800 ms were employed. The basicity of the amino moieties present in **1**, **2** and several reference aminoglycosides (including kanamycin-B, see Figures 6, 8, S4, S10, S11, S13, and S14), at 40 °C were derived by NMR. In order to unambiguously determine the pK_a's, carbon chemical shifts together with the heteronuclear $^1J_{HC}$ constants for the HC−N fragments, were also measured at different pH values from coupled ^{1}H−^{13}C HSQC experiments. This later parameter has been shown to be sensitive to the protonation state of the amino functions and is not affected by the ring current effect of the aromatic systems.[14] As a final control, the protonation state of **1** and **2** was checked in the presence of reference aminoglycoside kanamycin-B, employing equimolecular mixtures. In this way, any influence of the sample conditions on the pK_a perturbations detected could be ruled out.

Selective 1-D NOE experiments were recorded at different temperatures and pH values employing the 1D-DPFGSE NOE pulse sequence.[31]

MD Simulations. To get insights into the origin of the peculiar behavior deduced for the different aminoglycoside/aromatic complexes analyzed along the manuscript, we performed molecular dynamics (MD) simulations with the AMBER 10.0 package.[17] The conformational and dynamical properties of **1** (together with simpler disaccharide models) and **2** were tested assuming different protonation states of the aminoglycosides (see above). For highly flexible derivatives, such as **1**, the simulation lengths were adjusted to 0.1 μs in order to ensure an adequate sampling of the different conformational populations present in solution. In **2** the conformational fluctuations should be severely restricted by the aminoglycoside covalent scaffold. Consequently, simulation lengths were limited to 20 ns.

Two different treatments were employed for solvation. Thus, derivative **1** was analyzed in the presence of explicit TIP3P water,[18] counterions, periodic boundary conditions and Ewald sums for the treatment of long-range electrostatic interactions,[19] following a protocol identical to that previously described.[32] This methodology was rather expensive from a computational perspective, specially for 0.1 μs trajectories. However, it gave us the opportunity to determine the changes in the aminoglycoside solvation shells that accompany transitions between hairpin and disordered conformations. Indeed, this analysis provided valuable clues about the origin of the hairpin destabilization in protonated **1**.

For aminoglycoside **2** and simpler **1** models (**1a** and **1b**), MD trajectories were collected employing the Born model with the Bashford modification.[21] Continuous algorithms have been shown to provide reliable estimates of solvations energies at a reasonable computational cost. Moreover, lengthy equilibration periods are not required and the simulations are free from the artifacts derived from the use of periodic boundary conditions. Finally, this methodology is closely related to that used in the Quantum Mechanics analysis of simple aminocyclitol/aromatic complexes, described in the last section of the manuscript. Therefore, results derived employing both approaches could be easily compared.

In all cases, RESP atomic charges for the analyzed derivatives in the different protonation states considered, were derived by applying the RESP module of AMBER 10.0 package[17] to the HF/6-31G(d) ESP charges calculated with Gaussian 09.[22] The AMBER94 force field was implemented with GLYCAM04[33] and GAFF[34] parameters to accurately simulate the conformational behavior of these molecules. The time step was 1 fs in all of the simulations.

For derivative **2**, the theoretical chemical shift perturbations ($\Delta\delta$) induced at key aminocyclitol positions by the phenyl rings were calculated from the MD trajectories and compared with those measured experimentally. A set of 40 conformations (including 80 aminocyclitol/phenyl pairs) was extracted from each trajectory and the theoretical $\Delta\delta$ values, evaluated using the Johnson-Bovey model[35] as implemented in the program MOLMOL,[36] averaged over the entire ensemble.

Quantum Mechanics Calculations. The interaction energies of the different aminocyclitol/aromatic pairs considered were evaluated employing Quantum Mechanics calculations, assuming different protonation states of the aminocyclitol and different interaction geometries (including parallel and nonparallel stacking and NH_3^+/π interactions). Full geometry optimizations were carried out with the Gaussian 09 package[22] through the M06-2X functional recently developed by Thrular[23] and the triple-ζ TZVP basis set of

(31) Stott, K.; Stonehouse, J.; Keeler, J.; Hwang, T. L.; Shaka, A. J. *J. Am. Chem. Soc.* **1995**, *117*, 4199–4200.

(32) Corzana, F.; Busto, J. H.; Engelsen, S. B.; Jiménez-Barbero, J.; Asensio, J. L.; Peregrina, J. M.; Avenoza, A. *Chem.—Eur. J.* **2006**, *12*, 7864–7871.

(33) Woods, R. J.; Dwek, R. E.; Edge, C. J.; Fraser-Reid, B. *J. Phys. Chem. B* **1995**, *99*, 3832–3846.

(34) Wang, J.; Wolf, R. M.; Caldwell, J. W.; Kollman, P. A.; Case, D. A. *J. Comput. Chem.* **2004**, *25*, 1157–1174.

(35) Case, D. A. *J. Biomol. NMR* **1995**, *6*, 341–346.

(36) Koradi, R.; Billeter, M.; Wuthrich, K. *J. Mol. Graph.* **1996**, *14*, 51–55.

Ahlrichs.[24] Solvent effects were included in the optimization trough the integral equation formalism variant of the polarizable continuum model (IEF-PCM),[25] using UFF radii and the internally stored parameters for water, as implemented in Gaussian 09. Frequency analyses were carried out at the same level used in the geometry optimizations, and the nature of the stationary points was determined in each case according to the appropriate number of negative eigenvalues of the Hessian matrix. Gas-phase single-point energies at the spin-component scaled MP2 (SCS-MP2) level as proposed by Grimme[37] with the triple-ζ 6-311G(2d,p) basis set were calculated on the optimized geometries using Gamess (v.2009).[38] Basis set superposition errors (BSSE) were corrected by the Boys−Bernardi counterpoise method.[39] Solvation free energies (ΔG_{solv}) were calculated at the ab initio level through the conductor-like polarized continuum model (C-PCM),[26] which is based on the COSMO[40] method, using the internally stored parameters for water as implemented in Gamess. Counterpoise-corrected electronic energies were used for the discussion on the interaction energies between the fragments both in the gas phase (ΔEi_{gas}) and in solution ($\Delta Ei_{H_2O} = \Delta Ei_{gas} + \Delta G_{solv}$). Diverse contributions (electrostatic, exchange, repulsion, polarization and dispersion) to the interaction energies were calculated through the localized molecular orbital energy decomposition analysis (LMO-EDA)[27] as implemented in Gamess.

Acknowledgment. This investigation was supported by the Spanish "Plan Nacional" (MCYT) (Grant CTQ2007-67403/BQU) and the Comunidad de Madrid (Grant S2009/PPQ-1752). We also thank CESGA (Santiago de Compostela) for computer support.

Supporting Information Available: Experimental procedures for the synthesis of derivatives **1** and **2**. Characterization of synthetic intermediates and products. Figures S1−S17, showing details of the experimental and theoretical analysis of aminoglycoside/aromatic interactions described along the manuscript. Complete refs 17 and 22. This material is available free of charge via the Internet at http://pubs.acs.org.

JA1046439

(37) Grimme, S. *J. Chem. Phys.* **2003**, *118*, 9095–9102.
(38) (a) Schmidt, M. W.; Baldridge, K. K.; Boatz, J. A.; Elbert, S. T.; Gordon, M. S.; Jensen, J. H.; Koseki, S.; Matsunaga, N.; Nguyen, K. A.; Su, S. J.; Windus, T. L.; Dupuis, M.; Montgomery, J. A. *J. Comput. Chem.* **1993**, *14*, 1347–1363. (b) Gordon, M. S.; Schmidt, M. W. In *Theory and Applications of Computational Chemistry, the first forty years*; Dykstra, C. E., Frenking, G., Kim, K. S., Scuseria, G. E., Eds.; Elsevier: Amsterdam, 2005; Chapter 41, pp 1167−1189.
(39) Boys, S. F.; Bernardi, F. *Mol. Phys.* **1970**, *19*, 553–566.
(40) Klamt, A.; Schüürmann, G. *J. Chem. Soc. Perkin Trans 2* **1993**, 799–805.